REGULATION OF *IN SITU* TO INVASIVE BREAST CARCINOMA TRANSITION

Min Hu[1,2], Jun Yao[1,2], Danielle K. Carroll[2], Stanislawa Weremowicz[2,3], Haiyan Chen[4,5], Daniel Carrasco[1], Andrea Richardson[2,3], Mina J. Bissell[6], Shelia Violette[7], Rebecca S. Gelman[4,5], Stuart Schnitt[2,8], Kornelia Polyak[1,2]

Departments of [1]Medical Oncology and [4] Biostatistics and Computational Biology, Dana-Farber Cancer Institute, [3]Department of Pathology, Brigham and Women's Hospital, [2]Harvard Medical School, [5]Harvard School of Public Health, [8]Department of Pathology, Beth-Israel Deaconess Medical Center, Boston, MA 02115; [6]Lawrence Berkley National Laboratory, Berkeley, CA 94720; and [7]Biogen-Idec, Cambridge, MA 02142.

Running title: Myoepithelial cells as gatekeepers of breast tumor progression

Correspondence: Kornelia Polyak, Department of Medical Oncology, Dana-Farber Cancer Institute, 44 Binney Street, D740C, Boston, MA 02115; Phone: 617-632-2106; Fax: 617-582-8490; Email: Kornelia_Polyak@dfci.harvard.edu

SUMMARY

The transition of ductal carcinoma *in situ* (DCIS) to invasive carcinoma is a key event in breast tumor progression that is poorly understood. Comparative molecular analysis of tumor epithelial cells from *in situ* and invasive tumors has failed to identify consistent tumor stage-specific differences. However, the myoepithelial cell layer, present only in DCIS, is a key distinguishing and diagnostic feature. To determine the contribution of non-epithelial cells to tumor progression, we analyzed the role of myoepithelial cells and fibroblasts in the progression of *in situ* carcinomas using a xenograft model of human DCIS. Progression to invasion was promoted by fibroblasts, but inhibited by normal myoepithelial cells. The invasive tumor cells from these progressed lesions formed DCIS rather than invasive cancers when re-injected into naïve mice. Molecular profiles of myoepithelial and epithelial cells isolated from primary normal and cancerous human breast tissue samples corroborated findings obtained in the xenograft model. These results provide the proof of principle that breast tumor progression could occur in the absence of additional genetic alterations and that tumor growth and progression could be controlled by replacement of normal myoepithelial inhibitory signals.

SIGNIFICANCE

There has been a dramatic improvement in our ability to detect DCIS, but our understanding of the factors involved in its progression is poorly defined. Our data suggest that a key event of tumor progression is the disappearance of the normal myoepithelial cell layer due to defective myoepithelial cell differentiation provoked by microenvironmental signals. Thus, myoepithelial cells could be considered gatekeepers of the *in situ* to invasive carcinoma transition and understanding the pathways that regulate their differentiation may open new venues for cancer therapy and prevention.

INTRODUCTION

The natural history of most breast cancers involves progression through clinical and pathologic stages starting with ductal hyperplasia, progressing into *in situ* and invasive carcinomas, and culminating in metastatic disease (Allred et al., 2001; Burstein et al., 2004). DCIS is thought to be one of the precursors of invasive ductal carcinoma based on molecular, epidemiological, and pathological studies (Burstein et al., 2004; Simpson et al., 2005). Whereas there has been a dramatic improvement in our ability to detect DCIS, our understanding of the factors involved in its progression is far behind. Comprehensive gene expression and genetic studies comparing the profiles of DCIS and invasive ductal carcinomas have failed to identify *in situ* and invasive tumor-specific signatures (Chin et al., 2004; Ma et al., 2003; Porter et al., 2003; Porter et al., 2001; Yao et al., 2006). However, these studies have focused mainly on the tumor epithelial cells and the potential involvement of other epithelial and myoepithelial cells, and the stroma in tumor progression has not been explored in sufficient depth.

Epithelial-mesenchymal interactions are known to be important for the normal development of the mammary gland and for breast tumorigenesis (Howlett and Bissell, 1993). *In vivo* and *in vitro* studies have demonstrated that cells composing the microenvironment (myoepithelial and endothelial cells, fibroblasts, myofibroblasts, leukocytes, and other cell types) and the ECM molecules modulate tissue-specificity of the normal breast as well as the growth, survival, polarity, and invasive behavior of breast cancer cells (Bissell and Radisky, 2001; Elenbaas and Weinberg, 2001). In the normal mammary gland a layer of myoepithelial cells that produce, and are in contact with, the basement membrane surrounds luminal epithelial cells which in turn line the ducts and the alveoli. In addition to playing a role in expelling milk from the ducts during lactation due to their contractile function, myoepithelial cells are increasingly recognized as important regulators of normal mammary gland development and function due to their effect on luminal epithelial cell polarity, branching, and differentiation (Clarke et al., 2005; Gudjonsson et al., 2005; Gudjonsson et al., 2002a; Jolicoeur, 2005). Myoepithelial cells have also been labeled “natural tumor suppressors” due to their negative effects on tumor cells growth, invasion, and

angiogenesis achieved via secretion of protease inhibitors and downregulation of MMP (matrix metalloprotease) levels (Barsky and Karlin, 2005; Gudjonsson et al., 2005; Jones et al., 2003; Polyak and Hu, 2005). These conclusions have been largely based on *in vitro* co-culture assays; the role of myoepithelial cells in tumorigenesis *in vivo* is still poorly defined. The tumor-suppressive function of myoepithelial cells appear to get lost during the *in situ* to invasive carcinoma transition when both the organized myoepithelial cell layer and the basement membrane progressively disappear. The diagnostic criterion that distinguishes invasive from *in situ* carcinomas is the disappearance of the myoepithelial cell layer as an organized entity (Lerwill, 2004).

To explore the potential involvement of cells composing the microenvironment in tumor progression, we previously analyzed the gene expression and DNA methylation profiles of different cell types purified from normal breast tissue, DCIS, and invasive carcinomas and observed dramatic changes in all cells during tumor progression (Allinen et al., 2004; Hu et al., 2005). Importantly, myoepithelial cells associated with DCIS were not phenotypically normal; they had lost some of their differentiation markers and had up-regulated genes promoting angiogenesis and invasion (Allinen et al., 2004). While the physiological relevance of these molecular changes was unknown, based on our data we hypothesized that abnormal DCIS-associated myoepithelial cells, together with various stromal cells, degrade the basement membrane resulting in the progression of *in situ* carcinomas to invasive tumors. Testing this hypothesis requires an experimental model of DCIS that faithfully reproduces the human disease, since analysis of human tissue samples only allows correlative studies. The MCF10A1 human breast cell line series is one of the few human models of breast tumor progression (Lewis et al., 1999; Miller, 2000; Miller et al., 1993; Tait et al., 1996), although it is likely to reflect only a subset of breast tumors with basal-like features. A derivative of MCF10A1 cells is the MCF10ADCIS.com cell line (subsequently referred to as MCFDCIS) (Miller, 2000; Miller et al., 2000), which reproducibly forms comedo DCIS-like lesions that spontaneously progress to invasive tumors. This MCFDCIS xenograft model highly resembles human disease with respect to histopathology and natural history. Furthermore, here we show hat the gene

expression profiles of epithelial and myoepithelial cells purified from MCFDCIS xenografts are highly similar to that from primary human DCIS tumors. We used this model to explore the relative importance of myoepithelial cells and stromal fibroblasts in the *in situ* to invasive breast carcinoma transition. In this study we demonstrate that normal myoepithelial cells suppress, but fibroblasts enhance tumor growth and invasive progression in the absence of detectable genomic alterations in the tumor cells themselves. The gene expression profiles of DCIS-associated epithelial and myoepithelial cells isolated from primary human breast tissue samples correlated with the above findings and support the hypothesis that transition of *in situ* to invasive carcinoma is most likely regulated by loss of normal myoepithelial function leading to contact between tumor epithelial and stromal cells.

RESULTS

Characterization of the MCFDCIS cells and their xenografts

To explore whether the MCFDCIS provided a reasonable model for primary human DCIS, xenografts were analyzed for histology and molecular markers. We chose subcutaneous instead of orthotopic injections because tumors formed in the mammary fat pad became invasive regardless of conditions used presumably due to the invasion promoting effects of endogenous mouse fibroblasts (data not shown). Subcutaneous injections formed xenografts that were similar to human high-grade comedo DCIS. The duct-like structures were surrounded by basement membrane positive for laminin 5 and contained a layer of cells positive for myoepithelial markers (smooth muscle actin-SMA, CD10, and p63) (Figure 1A). Analysis of the tumors at different time points (3-8 weeks) after injection revealed a rapid progression from DCIS to invasive histology (Figure 1B). In DCIS, both SMA and p63 were expressed in the myoepithelial cell layer, whereas in invasive tumors, SMA-positive cells were stromal myofibroblasts, and a subset of tumor epithelial cells was p63 positive.

We tested several other breast cancer cell lines in xenograft assays, however, in none of these cases we were able to obtain tumors with DCIS histology (Figure S1 and data not shown) suggesting that this characteristic is unique for the MCFDCIS cells among the cells tested. We reasoned that this uniqueness may be due to their proposed bipotential progenitor properties (Santner et al., 2001). To test whether both epithelial and myoepithelial cells were derived from the human MCFDCIS cells and that the myoepithelial cell layer disappeared as tumors become invasive, we performed immuno-FISH (fluorescence *in situ* hybridization) analysis of MCFDCIS xenografts. Samples were collected at different time points after injection, using fluorescently labeled human and mouse cot-1 DNA as probes for FISH, pan-cytokeratin antibody (panCK) for staining of epithelial cells, and antibody to SMA to identify myoepithelial cells. As anticipated, panCK-positive tumor epithelial cells were indeed of human origin in all tumors (Figure S2). Interestingly, SMA-positive myoepithelial cells forming a layer around the duct-like structures were also of human origin (Figure 1C), confirming the bipotential progenitor property of

MCFDCIS cells. In contrast, SMA-positive myofibroblasts in the stroma were of mouse origin in all xenografts (Figure 1C). Immuno-FISH analysis also revealed the gradual disappearance of SMA-positive myoepithelial cells coinciding with the progression of DCIS to invasive tumors (Figure 1C). Since other MCF10 derivatives were also proposed to have progenitor properties (Santner et al., 2001), we tested these in xenograft assays as well, but they were either non-tumorigenic (MCF10AT cells) or formed invasive tumors (MCF10CA cells). Thus, of all the cells tested, the MCFDCIS cell line is the only human breast cancer cell line that forms DCIS xenografts.

To dissect the progenitor properties of the MCFDCIS cells, we analyzed the expression of known stem/progenitor and differentiated luminal epithelial and myoepithelial cell markers in cultured cells and in xenografts. Based on immunohistochemistry, MCFDCIS cells grown in 2D culture were uniformly positive for panCK, CK18, ESA, CDH1, CD44, CK17, CK5/6, p63 and VIM, partially positive for MUC1 and CK14, and negative for CD24, SMA, and CK19 (Figure 2A). FACS analysis showed that the cells were positive for ITGA6 and ITGB6, negative for CD10, and also confirmed the expression of ESA, CD44, CD24 and MUC1 (Figure S3A). In xenografts, most tumor epithelial cells were positive for panCK, ESA, CD44, CK17, CDH1, and VIM. In DCIS, p63 and SMA expression was limited to the myoepithelial cells which also showed decreased or no expression of MUC1, CD24, and CK18, while CK5/6 and CK14 demonstrated heterogeneous staining patterns with all cells positive in some areas and only the myoepithelial cells positive in other areas (Figure 2A). CK18, CD24, and MUC1 are thought to be specific for luminal epithelial cells (differentiated or committed progenitor), CD10 and SMA for myoepithelial cells, while CD44, CK17, CK5/6, p63, and VIM has been described as markers of basal/progenitor cells. Thus, based on our analyses *in vitro* cultured MCFDCIS cells have progenitor characteristics and in xenografts they differentiate into luminal and myoepithelial cells.

To determine if all or only a subpopulation of MCFDCIS cells have progenitor properties, we sorted the cells based on MUC1 expression into positive (MUC1+) and negative (MUC1-) fractions and injected them into mice. MUC1 expression has been used for identification of cells with progenitor properties

(Gudjonsson et al., 2002b; Stingl et al., 1998; Stingl et al., 2001; Stingl et al., 2005), and this was the only cell surface marker we found heterogeneously expressed in MCFDCIS cells in culture. Both MUC1+ and MUC1- cells gave rise to DCIS tumors (Figure S3B), suggesting that both populations have bipotential progenitor properties. We also derived single-cell clones of MCFDCIS cells with different CK14 and MUC1 expression levels based on immunocytochemistry (Figure 2B) and immunoblotting (Figure 2C). Four of these independent clones were injected into mice and resulting xenografts were analyzed for histology and expression of cell type-specific markers. Tumors derived from all four clones had a DCIS histology and showed the same CK14, MUC1, SMA, and p63 expression patterns (Figure 2D). Thus, using this approaches we found that all or a significant fraction of MCFDCIS cells may have bipotential progenitor properties, and the expression patterns of some genes (CK14, p63, MUC1, CD24, etc.) were discordant *in vitro* and *in vivo*.

Similarity of the MCFDCIS xenograft model to human DCIS at the molecular level

To ensure that results obtained using this model system are relevant to human disease, it is essential to establish if the MCFDCIS xenografts reproduce human disease. Thus, to compare genetic alterations in MCF10A1-series cells and MCFDCIS-derived xenografts to those found in sporadic human DCIS, we performed SNP (single nucleotide polymorphism) array analyses. All samples had a copy number gain at chromosome 8q24, including *C-MYC*, and homozygous deletion of *CDKN2A* at chromosome 9p21 (Figure S4A). The gain of 8q24 is a recurring genetic change observed in high-grade human DCIS tumors and homozygous deletion of *CDKN2A* has been described in a subset of breast carcinomas (Cairns et al., 1995; Yokota et al., 1999), supporting the similarity between the MCFDCIS model and human disease. The 8q24 copy number gain was confirmed by FISH; probes covering the MYC gene revealed two hybridization signals on chromosome 8q and one on chromosome 10q (Figure S4B) in all cells.

To define the similarity of MCFDCIS xenografts to human DCIS at the cellular lever, we purified luminal and myoepithelial cells using MUC1 and integrin beta 6 (ITGB6) as cell surface markers, respectively.

ITGB6 has recently been identified as a gene upregulated by p63 (Carroll et al., 2006); it is also induced by TGFβ1 (Zambruno et al., 1995) and involved in activation of latent-TGFβ1 (Munger et al., 1999). In MCFDCIS-derived DCIS xenografts, as well as in human DCIS, ITGB6 was specifically expressed in myoepithelial cells (Figure 1A), making it an ideal cell surface marker for their purification.

The purity of the MUC1+ and ITGB6+ cells was confirmed by semi-quantitative RT-PCR analysis of cell type-specific markers. Myoepithelial cell markers CD10 (*MME*), SMA (*ACTA2*), and p63 (*TP73L*) were present only in ITGB6+ cells (Figure 3A), consistent with their myoepithelial phenotype. Although the cells were separated based on their MUC1 and ITGB6 cell surface protein levels, the expression of *MUC1* and *ITGB6* mRNAs were not completely mutually exclusive in the two cell populations (Figure 3A).

Next we analyzed the comprehensive gene expression profiles of MUC1+ and ITGB6+ cells using SAGE. SAGE data further supported the myoepithelial and luminal epithelial characteristics of ITGB6+ and MUC1+ cells, since several known markers of these cell types were almost mutually exclusively expressed in the respective SAGE libraries (Table 1 and Supplemental Excel Spreadsheet 1). Furthermore, genes statistically significantly differentially expressed between ITGB6+ and MUC1+ cells were also differentially expressed between groups of "MYOEP" and "EPI" cells derived from human breast tissue (Table 1 and Supplemental Excel Spreadsheet 1). Hierarchical cluster analysis of the relatedness of the various cell types also confirmed the myoepithelial and epithelial characteristics of ITGB6+ and MUC1+ cells, respectively (Figure 3B). Interestingly, ITGB6+ cells cluster between normal and DCIS associated myopithelial cells, thus, phenotypically they are not normal myoepithelial cells, consistent with their origin from the MCFDCIS tumorigenic cell line.

Functional annotation of the genes differentially expressed between ITGB6+ and MUC1+ cells revealed statistically significant enrichment of genes involved in ECM, basement membrane, development, muscle development, and angiogenesis in ITGB6+ cells (Figure 3C). Both cell types showed high expression of genes related to ectoderm and epidermis development, while MUC1+ cells were enriched for plasma membrane proteins and genes regulating ion homeostasis (Figure 3C).

SAGE data indicated specific activation of the TGFβ1 and hedgehog (Hh) signaling pathways in ITGB6+ cells as well as in human DCIS myoepithelial cells (Table 1). Both of these pathways have been implicated in the regulation of progenitor cell function and myoepithelial differentiation. Thus, to dissect the possible mechanism of their cell type-specific activation, we analyzed the expression of their signaling components by semi-quantitative RT-PCR in MUC1+ and ITGB6+ cells. *TGFBR1* and *TGFBR2* (receptors for TGFβ1) and *PTCH1*, *PTCH2*, and *SMO* (receptors for Hh ligands) were equally present in both cell populations whereas *SMAD2*, *SMAD3*, and *GLI2* (transcription factors), *IHH* (a ligand for PTCH), and TGFβ1 transcriptional targets *SMAD7* and *TGFBI,* were expressed more abundantly in ITGB6+ cells (Figure 3A). These data suggest that specific activation of TGFβ1 targets in ITGB6+ cells may be due to the restricted expression of SMAD2 and SMAD3 in these cells, a finding that was confirmed also by immunohistochemical analysis of DCIS xenografts (data not shown). Hh signaling and *GLI2* expression may be preferentially upregulated in ITGB6+ cells due to their high expression of *IHH* (Figure 3A) and *BGN* (Table 1), a proteoglycan recently implicated in Hh responses (Rubin et al., 2002). The TGFβ1 and Hh signaling pathways and p63 are all known to play important roles in the regulation of epithelial stem cell function and their differentiation (Liu et al., 2006; Liu et al., 2005; McKeon, 2004; Mishra et al., 2005) and the combination of all of them may be required for defining myoepithelial and luminal epithelial cell phenotypes.

Potential mechanism underlying basement membrane degradation and progression to invasion

The gene expression profiles of ITGB6+ and myoepithelial cells isolated from primary human normal and DCIS breast tissue suggested that one of their main functions is the synthesis and maintenance of the basement membrane (BM). Degradation of the basement membrane is a hallmark of malignancy and the definition of invasive progression. Despite the importance of this issue, the molecular mechanism underlying BM degradation is undefined. Several MMPs have been implicated to play a role in this process, but a recent study concluded that the MMPs that most likely to degrade BM *in vivo* are MMP14,

MMP15, and MMP16 (Hotary et al., 2006). To determine if upregulation of these three MMPs during breast tumor progression may explain *in situ* to invasive carcinoma progression, and to identify the cell type that may express them, we analyzed their expression in our SAGE data on various cell types isolated from normal breast tissue and *in situ* and invasive carcinomas (Allinen et al., 2004). This analysis showed that MMP14 was highly expressed in myoepithelial cells and myofibroblasts, and its expression significantly increased in DCIS-associated myoepithelial cells compared to normal ones (data not shown). This expression pattern was consistent with the hypothesis that MMP14 may be involved in BM degradation and also that its upregulation in DCIS myoepithelial cells contribute to invasive progression. To confirm the SAGE data, we analyzed the expression of MMP14 by real-time PCR in epithelial and myoepithelial cells purified from multiple independent cases of normal breast tissue, and *in situ* and invasive tumors, together with bulk tumor samples. High MMP14 expression was detected in myoepithelial cells, with highest levels in DCIS-associated myoepithelium (Figure 3D). The high MMP14 levels seen in bulk invasive tumor tissue was due to its expression in myofibroblasts since tumor epithelial cells and myofibroblasts had low and high levels of MMP14, respectively (Figure 3D and data not shown). Next, we tested the expression of MMP14 in MUC1+ and ITGB6+ cells isolated from MCFDCIS xenografts and found that MMP14 was highly expressed in ITGB6+ cells (Figure 3E) correlating with their myoepithelial phenotype and strengthening the similarity between our model and human DCIS. The high expression of MMP14 in ITGB6+ cells in the MCFDCIS xenografts also indicates that these cells are more similar to DCIS-associated than normal myoepithelial cells and could also explain why they are not able to permanently inhibit progression to invasion.

The effect of co-injected myoepithelial cells and fibroblasts on tumor growth and progression

Following the verification that the MCFDCIS xenograft model reproduces main aspects of human DCIS tumors, we used this model to test the role of non-epithelial cells in tumor progression. Thus, we injected MCFDCIS cells into nude mice alone or together with normal spontaneously immortalized HME50 (Shay

et al., 1995), E6/E7-immortalized D920 494/3 (Gudjonsson et al., 2002a), or primary cultured myoepithelial cells, or primary cultured fibroblasts derived from normal breast tissue (PBS), invasive ductal carcinomas (PBTS), rheumatoid arthritis (RASF), skin, or osteoarthritis (OASF). All xenografts were analyzed at early (3-4 weeks) time-points after injection in order to avoid spontaneous progression to invasive tumors. Normal myoepithelial cells statistically significantly suppressed tumor weight; fibroblasts from normal breast, skin, and osteoarthritis had no measurable effect; and fibroblasts from breast tumors and rheumatoid arthritis increased tumor weight (Figure 4A and data not shown). Microscopic examination revealed dramatic differences in histology among the different co-injection groups. MCFDCIS cells alone or co-injected with normal myoepithelial cells formed DCIS whereas co-injection of any fibroblasts resulted in invasive carcinomas (Figure 4B and data not shown). The DCIS and invasive histology was confirmed by the immunohistochemical analysis of myoepithelial markers (Figure 3B). Analysis of the expression of MIB1 (Ki67), a commonly used cell proliferation marker, revealed increased proliferation in invasive tumors (Figure 4B), correlating with their faster growth rate (data not shown). All of these experiments were performed at least three times with essentially the same results using myoepithelial cells and fibroblasts derived from multiple independent patients. The tumor growth-suppressing effect of normal myoepithelial cells was not specific for the MCFDCIS cell line, since similar results were obtained when myoepithelial cells were used with other breast cancer cell lines (MCF7, MDA-MB-231, MDA-MB-435, and SK-BR-3) for co-injections (data not shown).

To determine the species of origin and localization of various cell types in the xenografts, immuno-FISH experiments were performed on representative tumors from each experimental group. Consistent with prior studies describing the lack of long-term survival of human primary (not immortalized) stromal cells in xenografts in immunodeficient mice (Kuperwasser et al., 2004), we were not able to detect human fibroblasts in the stroma in any of the tumors (Figure 4C-D). All SMA-positive myofibroblasts in the stroma were mouse origin, while cytokeratin positive epithelial and SMA-positive myoepithelial cells, present only in DCIS tumors, were human. We repeated these experiments in NOD/SCID mice, a more

severely immunodeficient mouse strain in which human stromal cells have been reported to survive longer (Kuperwasser et al., 2004), but even in these tumors, we detected only occasional human fibroblasts in the stroma (data not shown). Thus, despite their inability to persist long-term in immunodeficient mice, co-injected fibroblasts exert a long-lasting effect on tumor weight and histology. The lack of requirement for their long-term survival was demonstrated also by the use of lethally irradiated fibroblasts for co-injections, which also resulted in invasive tumors and an even more pronounced increase in tumor weight (data not shown).

We also analyzed xenografts obtained from the co-injection of all three cell types: MCFDCIS tumor cells, normal myoepithelial cells, and fibroblasts. Interestingly, inclusion of normal myoepithelial cells was able to reverse the tumor growth and progression-promoting effects of all fibroblasts, since tumors derived from triple-injections were smaller and had DCIS histology (Figure 4E-F).

To determine if the tumor growth and progression-promoting effects of co-injected human fibroblasts were due to the preferential outgrowth of a minority subpopulation of MCFDCIS cells with preexisting or acquired alterations leading to invasion, we isolated tumor epithelial cells from xenografts formed from MCFDCIS cells alone and from different co-injections, and re-injected them (without adding any non-epithelial cells) into new (naïve) nude mice. All re-injected tumors had DCIS histology, suggesting that the MCFDCIS epithelial cells were similar in all tumors and that fibroblasts have to be present at the time of injection to exert their progression-promoting effects (Figure 4G). SNP array analysis of xenografts formed from MCFDCIS cells at different time points (3-8 weeks) and from the different co-injection groups also demonstrated that all xenografts, with the exception of two tumors, were indistinguishable from the parental MCFDCIS cells (Figure S4C). Thus, acquisition of additional genetic alterations is not necessary for progression to invasive tumors.

The role of COX2 in epithelial-stromal interactions and tumorigenesis

COX2 has been implicated in early stages of breast tumorigenesis, the regulation of mammary epithelial cell immortalization and proliferation, and epithelial-stromal cell interactions (Crawford et al., 2004; Sato et al., 2004; Shim et al., 2003). To evaluate the expression of COX2 in our model system we performed immunohistochemical analysis of representative tumors from each experimental group. The level of COX2 was fairly low and heterogeneous in MCFDCIS and MCFDCIS+HME tumors, whereas co-injection of fibroblasts led to its dramatic up-regulation in tumor epithelial cells (Figure 5A). This observation is consistent with studies reporting heterogeneous COX2 expression in human breast tumors (Leo et al., 2006) and a recent finding in pancreatic cancer where COX2 expression is markedly augmented in tumor cells in response to co-culture with fibroblasts, and downregulation of COX2 decreased the invasive properties of cancer cells acquired through epithelial-mesenchymal interactions (Sato et al., 2004). However, in contrast to this *in vitro* pancreatic cancer study, we did not see upregulation of COX2 in the stromal cells of any of the xenografts (data not shown). The MCFDCIS cell alone xenografts were mostly negative for COX2 expression even at later time points (7-8 weeks) after injection when all the tumors were invasive (data not shown). Thus, upregulation of COX2 in tumor epithelial cells is not a consequence of the cell-autonomous invasive phenotype, but due to the co-injected human fibroblasts.

COX2 is known to contribute to tumor cell invasion and angiogenesis (Mann et al., 2005; Singh et al., 2005). To investigate the association between COX2 expression and markers of invasion and angiogenesis, we analyzed the mRNA levels of COX2 (*PTGS2*), *MMP9*, *MMP13, MMP14, MMP15, MMP16*, *VEGFA*, *VEGFC*, and *CXCL12* by quantitative RT-PCR in representative tumors from each experimental group. Overall, co-injection of normal myoepithelial cells decreased while that of fibroblasts increased the expression of most angiogenesis and invasion-related genes analyzed, but the observed differences were not always statistically significant (Figure 5B and data not shown). Interestingly, the

expression of MMP14 (MT1-MMP) was consistently upregulated in all of the invasive xenografts consistent with its proposed role in the degradation of basement membrane (Hotary et al., 2006).

Based on these observations we hypothesized that upregulation of COX2 in the tumor epithelial cells by co-injected fibroblasts may be responsible for their tumor growth and progression-promoting effects, and, thus, these may be abolished or decreased by inhibition of COX2 activity. To test this hypothesis, we analyzed the consequences of treatment with celecoxib, a COX2-specific inhibitor, on the weight and histology of xenografts derived from MCFDCIS cells injected alone or together with RASF inflammatory fibroblasts. Feeding the mice with a celecoxib-containing diet had no significant effect on the growth of MCFDCIS cells alone xenografts, but it completely eliminated the tumor-growth promoting effects of the co-injected RASF fibroblasts (Figure 5C) and partially inhibited DCIS progression to invasive tumors (Figure 5D). Therefore at least part of the tumor progression promoting effects of the stroma is mediated via COX2. Tumor suppression by celecoxib are unlikely to be due to its anti-inflammatory properties, since we did not detect infiltrating inflammatory cells (CD45+ cells) in any of the xenografts (data not shown).

Dual role for the basement membrane in tumor progression

Our gene expression data of epithelial and myoepithelial cells purified from MCFDCIS xenografts and human primary tissue samples suggested the preferential activation of the TGFβ1 and p63 pathways in myoepithelial cells (Table 1). Prior studies in keratinocytes demonstrated that TGFβ1 influences p63 expression (Waltermann et al., 2003). Thus, we asked whether treatment with TGFβ1 influences p63 protein levels or activity in MCFDCIS cells in which the predominant p63 isoform is ΔNp63α based on immunoblot and RT-PCR analyses (data not shown). MCFDCIS cells grown in 2D or in suspension cultures were analyzed at different time points following TGFβ1 treatment for the expression of p63 and for common targets of the two pathways. TGFβ1 did not effect p63 protein levels in any conditions analyzed, however, loss of ECM contact itself resulted in dramatic loss of p63 protein levels (Figure 6A),

consistent with prior studies in MCF-10A cells (Carroll et al., 2006). The basal levels of integrin β6 and vimentin were slightly higher in suspended cells, whereas the induction of vimentin by TGFβ1 was less pronounced in suspension than in attached cells (Figure 6A). Thus, whereas TGFβ1 did not influence p63 protein levels, cell-ECM interaction appears to dramatically influence both signaling pathways, with p63 expression and thus the basal/myoepithelial phenotype being absolutely dependent on ECM contact.

p63 has been shown to play an essential role in the regulation of epithelial stem cell function and differentiation (McKeon, 2004). To determine if constitutive overexpression of p63 would influence luminal and myoepithelial cell differentiation and the phenotype of the DCIS xenografts, we generated derivatives of MCFDCIS cells overexpressing ΔNp63α or TAp63γ. Functional overexpression of ΔNp63α was confirmed by immunoblot analysis of its expression as well as that of its transcriptional targets ITGB6, laminin 5, and vimentin (Figure 6B). Both ITGB6 and laminin 5 mediate cell-ECM interactions and their upregulation is consistent with the recent finding that p63 regulates epithelial survival and cell adhesion (Carroll et al., 2006). Despite several attempts, we were unable to obtain MCFDCIS derivatives with constitutive TAp63γ overexpression (Figure 6B and data not shown). Similarly decreasing p63 expression in MCFDCIS cells using shRNA resulted in cell death (data not shown). Injection of control and ΔNp63α-overexpressing MCFDCIS cells into mice revealed no significant difference in tumor growth and histology between the two experimental groups (Figure 6C and data not shown). Intriguingly, despite the overexpression of ΔNp63α in MCFDCIS cells prior to injection, in the resulting xenografts p63 was only detected in myoepithelial cells (Figure 6C), suggesting its post-transcriptional downregulation in luminal epithelial cells, potentially due to lack of contact with basement membrane. Thus, the basement membrane appears to have a dual role in the inhibition of *in situ* to invasive carcinoma transition: it serves as barrier separating epithelial and myoepithelial cells from the stroma, and it is also required for the differentiation and maintenance of myoepithelial cells (Figure 6D).

DISCUSSION

The DCIS to invasive carcinoma transition is a clinically important, but poorly understood step of breast tumorigenesis (Allred et al., 2001; Burstein et al., 2004). We and others have analyzed the gene expression and genetic profiles of tumor epithelial cells isolated from DCIS and invasive tumors, but have not been able to define a tumor stage-specific molecular event (Chin et al., 2004; Ma et al., 2003; Porter et al., 2003; Porter et al., 2001; Yao et al., 2006). At the same time, the importance of changes in the microenvironment during tumor progression has been increasingly recognized (Bissell and Radisky, 2001; Ronnov-Jessen et al., 1996; Tlsty and Hein, 2001; Weinberg and Mihich, 2006). Myoepithelial cells were shown to be responsible for formation of polarized breast acini in 3-dimensional cultures (Gudjonsson et al., 2002a), and focal disruption of basement membrane appears to coincide with the disappearance of myoepithelial cells and stromal changes in human DCIS with high risk of progression to invasive carcinoma (Man et al., 2003). Correlating with the disappearance of the myoepithelial cells during the *in situ* to invasive carcinoma transition, the gene expression and epigenetic profiles of myoepithelial cells associated with DCIS become distinct from those in normal breast (Allinen et al., 2004; Hu et al., 2005). The signals that initiate these changes are unknown, although paracrine interactions with neoplastic epithelial and a variety of stromal cells are potential candidates. In contrast to normal myoepithelial cells, tumor-associated fibroblasts and myofibroblasts have been shown to promote tumorigenesis via enhancing angiogenesis, and proliferation, survival, invasive, and metastatic behavior of tumor epithelial cells (Bissell and Radisky, 2001; Ronnov-Jessen et al., 1995; Tlsty and Hein, 2001; Weinberg and Mihich, 2006). We therefore tested the hypothesis that myoepithelial cells and fibroblasts regulate the *in situ* to invasive carcinoma transition using a xenograft model of human DCIS based on the MCFDCIS cell line.

The MCFDCIS cells form DCIS-like xenografts that progress to invasive carcinomas with time. Based on co-injection experiments, we demonstrated that in the absence of normal myoepithelial cells and regardless of their tissue of origin, fibroblasts promoted progression of DCIS to invasive tumors and

upregulated COX2 expression in tumor epithelial cells. Additionally, breast tumor-associated and even more dramatically rheumatoid arthritis synovium-associated fibroblasts, also increased tumor growth, at least in part due to their induction of COX2 in tumor epithelial cells, since treatment with COX2 inhibitor diminished this effect. Upregulation of COX2 has been implicated in breast tumor initiation and metastatic progression, but this is still controversial. Our analysis of COX2 expression in primary breast tumors and breast cancer cell lines did not reveal consistent overexpression compared to normal epithelial cells (Zhao *et al.* submitted). Similarly, a recent study did not detect significant increase in COX2 protein levels during tumor progression (Leo et al., 2006). Thus, deciphering the role of COX2 in breast tumor progression requires further studies.

Co-injection of normal myoepithelial cells overcame the tumor progression-promoting effects of fibroblasts and effectively suppressed tumor weight. Most importantly, these differences in tumor growth and histology were not caused by permanent changes in the epithelial cells of the tumors: based on SNP array analysis and only with a couple of exceptions, all xenografts were genetically identical to the parental MCFDCIS cells. Furthermore, MCFDCIS cells retrieved from invasive tumors were still able to form DCIS when re-injected into naïve mice in the absence of additional fibroblasts.

We found that the unique ability of the MCFDCIS cells to form DCIS is due to their bipotential progenitor property that allows them to differentiate into luminal epithelial and myoepithelial cells *in vivo.* Differentiation to the myoepithelial cell phenotype is required for DCIS histology, and this process is influenced by co-injected normal myoepithelial cells and fibroblasts presumably via paracrine factors including laminin 1 (Gudjonsson et al., 2002a). Our gene expression profiling of immortalized normal myoepithelial cells and fibroblasts used for co-injections identified many candidate molecules that could mediate these interactions *in vivo* (data not shown). Most likely, a combination of these factors is necessary to influence the differentiation of bipotential progenitors into distinct lineages.

Based on our immunohistochemical analyses and gene expression profiling of luminal (MUC1+) and myoepithelial (ITGB6+) cells isolated from DCIS xenografts, we identified p63, Hh, and TGFβ1

signaling pathways as potential regulators of the luminal and myoepithelial cell phenotypes. Many of the targets of these pathways encode ECM proteins and receptors, and several of these are regulated by more than one signaling pathway. For example, both p63 and TGFβ1 upregulate ITGB6 expression which in turn can activate latent-TGFβ1, generating a positive feed-back loop. At the same time, p63 protein levels are regulated by cell-ECM interactions, and luminal epithelial differentiation may be initiated by detachment from basement membrane and subsequent downregulation of p63. Thus, the integrity of the basement membrane may be key to the maintenance of the basal/myoepithelial cell layer. We believe the proteases secreted by tumor epithelial and the other cells in the microenvironment promote tumor progression via destroying the basement membrane and inhibiting progenitor to myoepithelial cell differentiation. Previously it was shown that destruction of basement membrane by MMP3 in transgenic mice was accompanied with formation of aberrant stroma and eventual mammary tumors (Sternlicht et al., 1999; Thomasset et al., 1998). Furthermore destruction of basement membrane by MMP3 in a non-malignant mouse mammary cell line in culture was shown to accompany acquisition of genomic instability (Radisky et al., 2005). Consistent with these, we found dramatic up-regulation of MMP14 in DCIS associated myoepithelial cells in human tissue samples and in the ITGB6+ myoepithelial cells in MCFDCIS xenografts. Furthermore, gene ontology analysis of genes differentially expressed between epithelial and myoepithelial cells isolated from primary human tissue samples as well as from MCFDCIS xenografts, demonstrated that myoepithelial cells play important roles in basement membrane synthesis and degradation. The phenotypic changes that occur in these cells in DCIS lead to progressive degradation of the basement membrane, which eliminates the barrier between the epithelial and stromal cell compartments and also results in the loss of myoepithelial cells. Human DCIS has been shown to have numerous genetic alterations and is almost indistinguishable from the invasive tumors (Chin et al., 2004). As such additional mutations are not necessary for the *in situ* to invasive transition; loss of the basement membrane, epithelial cell organization and polarity due to disappearance of myoepithelial cells, appears to be sufficient to pave the way for tumor progression and invasion. A simplified view of these dynamic

cellular and signaling interactions and their effect on the DCIS to invasive carcinoma progression are summarized in Figure 6D. Breast tumors are very heterogeneous with several distinct molecular subtypes and potentially distinct tumor progression pathways. MCFDCIS cells resemble basal-like breast tumors that thought to originate from bipotential stem cells (Yehiely et al., 2006). Specifically, the ITGB6+ myoepithelial cells are derived from MCFDCIS cells, thus, they are genetically abnormal contrary to myoepithelial cells isolated from human non-basal DCIS (Allinen et al., 2004). Thus, our model may not be universally true for all breast tumors and there are possibly other pathways of progression to invasive breast carcinoma.

In summary, our data suggest that the progression of *in situ* to invasive breast carcinoma may not be due to the intrinsic properties of the tumor epithelial cells acquired during tumor evolution, but determined by complex interactions among all the cell types that compose the tumor microenvironment. Our conclusions are based on a xenograft model of human DCIS and the characterization of individual cell types isolated from primary human breast tissue samples. Our model is also consistent with clinical and pathology data in human patients as well as with data from animal models of breast cancer. Thus, our results not only highlight the importance of the microenvironment in tumor progression, but also point to the significance of the myoepithelial cell layer as the gatekeeper of DCIS. Furthermore, the results suggest that therapeutic strategies targeting interactions of tumor epithelial cells with their surroundings may be more beneficial to inhibiting tumor progression than focusing on the tumor cells alone.

EXPERIMENTAL PROCEDURES

Cells and tissue specimens

MCF10A1 and its derivative cells were obtained from Dr. Fred Miller (Karmanos Cancer Institute, Detroit, MI). Immortalized myoepithelial cells HME50 (Shay et al., 1995) and D920 494/3 (Gudjonsson et al., 2002a) were generously provided by Drs. Jerry Shay (UT Southwestern, Dallas, TX) and Mina Bissell (Lawrence Berkeley National Laboratory, CA), respectively. RASF and OASF were generous gifts by Drs. Steve Goldring (Beth-Israel Deaconess Medical Center, Boston, MA) and John D. Mountz (University of Alabama, Birmingham, AL). Skin fibroblasts were purchased from Coriell Institute for Medical Research (Camden, NJ) and American Type Culture Collection (Manassas, VA). Primary cultured myoepithelial cells and primary breast normal or tumor stroma were purified from tissue samples from the Brigham and Women's Hospital (Boston, MA) as previously described (Allinen et al., 2004). All human tissue was collected using protocols approved by the Institutional Review Boards; informed consent was obtained from each individual who provided tissues with linked clinical data. Cells were grown in the media recommended by the providers. MCF10A series cells were cultured in DMEM/F12 (Invitrogen, Carlsbad, CA) supplemented with 5% horse serum, EGF, insulin, cholera toxin, and hydrocortisone (all from Sigma, St. Louis, MI); myoepithelial cells were maintained in MEGM (Cambrex, Walkersville, MD), while fibroblasts were kept in DMEM (Invitrogen, Carlsbad, CA) with 10% iron fortified bovine calf serum (Hyclone, Logan, UT). Generation of VSV-G pseudotyped retroviruses expressing human ΔNp63α and TAp63γ cDNAs and retroviral infection of MCFDCIS cells were carried out as previously described (Carroll et al., 2006). Cells were selected and maintained in 2 μg/ml and 1 μg/ml puromycin, respectively.

Mouse xenograft experiments

For xenograft studies 100,000 MCFDCIS cells were injected subcutaneously into 6-9 week old female nude mice alone or together with 2-3 fold excess of HME, RASF, PBS, or PBTS cells in 50% Matrigel

(BD Biosciences, Bedford, MA). Tumors were allowed to grow for 3-8 weeks. Xenografts were weighed and then either snap frozen on dry ice and stored at -80^{o}C for DNA/RNA purification, formalin fixed and paraffin embedded, or processed for cell sorting. For celecoxib experiments, mice were fed with a control AIN-93G diet (Dyets, Inc., Bethlehem, PA) or an AIN-93G diet with 0.9 g/kg celecoxib (LKT Laboratories, St. Paul, MN) starting 7-10 days before injection and continued for the duration of the experiment.

Immunohistochemistry, immunocytochemistry, immunoblot, and FACS analyses

The list of antibodies used is provided in the Supplemental Table 1. Immunohistochemistry, immunoblot, and FACS analyses were performed as recommended by the suppliers and essentially as previously described (Allinen et al., 2004; Polyak et al., 1994). For immunocytochemistry, cells were fixed with HistoChoice Tissue Fixative (Amresco, Solon, OH), and permeablized with 0.5% Triton X-100. Cells were blocked and incubated with primary antibodies, followed by biotin-conjugated secondary antibodies, ABC kit (Vector Labs, Burlingame, CA), and DAB Peroxidase Substrate (Sigma, St. Louis, MI).

FISH, immuno-FISH, and SNP array analysis

For MYC FISH LSI C-MYC (Spectrum Orange), LSI MYC Dual Color Break Apart Probe (5' Spectrum Orange, 3' Spectrum Green), CEP8 (Spectrum Aqua and Spectrum Green), and CEP10 (Spectrum Aqua) probes were purchased from Vysis, Inc. (Downers Grove, IL). Cells were treated with colcemid, harvested, and used for metaphase chromosome spreads preparations according to standard protocols. Hybridization of metaphase chromosomes was performed as previously described (Ney et al., 1993). Slides were examined using a fluorescence microscope equipped with a CytoVysion capturing system. Immuno-FISH was performed following previously described procedures (Peters et al., 2005), but using CK and SMA antibodies and Cot1 DNA. SNP array analysis was performed by the Dana-Farber

Microarray Core using Affymetrix 11K XbaI SNP arrays and protocols recommended by Affymetrix (Santa Clara, CA) essentially as described previously (Allinen et al., 2004).

Cell purification, SAGE, PCR, and statistical analyses

Cell purification and SAGE library generation and analyses were performed as described previously (Allinen et al., 2004), except that MUC1 (clone DF3) and ITGB6 (clone 3G9) antibodies were used. Gene ontology enrichment scores for the SAGE libraries were calculated as –log(p-value) by comparing the significantly highly expressed genes in the two cell types analyzed to the background (all genes in the two libraries) with one-sided Fisher test. Details of the clustering analysis are described in the Supplemental Data. cDNA synthesis, and quantitative and semi-quantitative RT-PCR were carried out essentially as described (Allinen et al., 2004; Hu et al., 2005; Yao et al., 2006). A list of primers used for PCR analyses is available upon request. Xenografts weights and relative gene expression levels were analyzed using a two-sided exact Wilcoxon Rank Sum test stratified by experiment when the data from different experiments were combined. In mouse xenograft experiments when both sides of the mouse got the same injection and the weights of the two tumors correlated, the average of the two tumor weights was used as the end point. There were no corrections for multiple comparisons.

ACKNOWLEDGEMENTS

We greatly appreciate the help of Diana Calogrias with the acquisition of human tissue samples and Natasha Pliss with immunohistochemistry. We thank Drs. John Mountz (University of Alabama, Birmingham, AL) and Steven Goldring (Beth-Israel Deaconess Medical Center, Boston, MA) for providing us with primary cultures derived from osteoarthritis and rheumatoid arthritis cases, Dr. Paul Weinreb (Biogen-Idec, Cambridge, MA) for his help with ITGB6 assays, Dr. Ole Petersen (Panem Institute, Denmark) for the D920 myoepithelial cells, Drs. Craig Allred, Bert Vogelstein, and Myles Brown, and Lauren Campbell for their critical reading of the manuscript, and the Genome Sciences

Centre, British Columbia Cancer Agency, Vancouver Canada for SAGE library sequencing. This work was supported in part by NIH (CA89393, CA94074, and CA116235), DOD (DAMD17-02-1-0692 and W8IXWH-04-1-0452), ACS (RSG-05-154-01-MGO) grants to KP, Susan G. Komen Foundation fellowship (PDF042234) to MH, and by Biogen-Idec. Work from the MJB laboratory was supported by NIH (CA64786) to MJB and Ole Petersen.

COMPETING FINANCIAL INTERESTS STATEMENT

KP receives research support from and is a consultant to Novartis Pharmaceuticals, Inc. KP also receives research support from Biogen-Idec and is a consultant to Aveo Pharmaceuticals, Inc.

REFERENCES

Allinen, M., Beroukhim, R., Cai, L., Brennan, C., Lahti-Domenici, J., Huang, H., Porter, D., Hu, M., Chin, L., Richardson, A.*, et al.* (2004). Molecular characterization of the tumor microenvironment in breast cancer. Cancer Cell *6*, 17-32.

Allred, D.C., Mohsin, S.K., and Fuqua, S.A. (2001). Histological and biological evolution of human premalignant breast disease. Endocr Relat Cancer *8*, 47-61.

Barsky, S.H., and Karlin, N.J. (2005). Myoepithelial cells: autocrine and paracrine suppressors of breast cancer progression. J Mammary Gland Biol Neoplasia *10*, 249-260.

Bissell, M.J., and Radisky, D. (2001). Putting tumours in context. Nat Rev Cancer *1*, 46-54.

Burstein, H.J., Polyak, K., Wong, J.S., Lester, S.C., and Kaelin, C.M. (2004). Ductal carcinoma in situ of the breast. N Engl J Med *350*, 1430-1441.

Cairns, P., Polascik, T.J., Eby, Y., Tokino, K., Califano, J., Merlo, A., Mao, L., Herath, J., Jenkins, R., Westra, W., and et al. (1995). Frequency of homozygous deletion at p16/CDKN2 in primary human tumours. Nat Genet *11*, 210-212.

Carroll, D.K., Carroll, J.S., Leong, C.O., Cheng, F., Brown, M., Mills, A.A., Brugge, J.S., and Ellisen, L.W. (2006). p63 regulates an adhesion programme and cell survival in epithelial cells. Nat Cell Biol *8*, 551-561.

Chin, K., de Solorzano, C.O., Knowles, D., Jones, A., Chou, W., Rodriguez, E.G., Kuo, W.L., Ljung, B.M., Chew, K., Myambo, K.*, et al.* (2004). In situ analyses of genome instability in breast cancer. Nat Genet *36*, 984-988.

Clarke, C., Sandle, J., and Lakhani, S.R. (2005). Myoepithelial cells: pathology, cell separation and markers of myoepithelial differentiation. J Mammary Gland Biol Neoplasia *10*, 273-280.

Crawford, Y.G., Gauthier, M.L., Joubel, A., Mantei, K., Kozakiewicz, K., Afshari, C.A., and Tlsty, T.D. (2004). Histologically normal human mammary epithelia with silenced p16(INK4a) overexpress COX-2, promoting a premalignant program. Cancer Cell *5*, 263-273.

Elenbaas, B., and Weinberg, R.A. (2001). Heterotypic signaling between epithelial tumor cells and fibroblasts in carcinoma formation. Exp Cell Res *264*, 169-184.

Gudjonsson, T., Adriance, M.C., Sternlicht, M.D., Petersen, O.W., and Bissell, M.J. (2005). Myoepithelial cells: their origin and function in breast morphogenesis and neoplasia. J Mammary Gland Biol Neoplasia *10*, 261-272.

Gudjonsson, T., Ronnov-Jessen, L., Villadsen, R., Rank, F., Bissell, M.J., and Petersen, O.W. (2002a). Normal and tumor-derived myoepithelial cells differ in their ability to interact with luminal breast epithelial cells for polarity and basement membrane deposition. J Cell Sci *115*, 39-50.

Gudjonsson, T., Villadsen, R., Nielsen, H.L., Ronnov-Jessen, L., Bissell, M.J., and Petersen, O.W. (2002b). Isolation, immortalization, and characterization of a human breast epithelial cell line with stem cell properties. Genes Dev *16*, 693-706.

Hotary, K., Li, X.Y., Allen, E., Stevens, S.L., and Weiss, S.J. (2006). A cancer cell metalloprotease triad regulates the basement membrane transmigration program. Genes Dev *20*, 2673-2686.

Howlett, A.R., and Bissell, M.J. (1993). The influence of tissue microenvironment (stroma and extracellular matrix) on the development and function of mammary epithelium. Epithelial Cell Biol *2*, 79-89.

Hu, M., Yao, J., Cai, L., Bachman, K.E., van den Brule, F., Velculescu, V., and Polyak, K. (2005). Distinct epigenetic changes in the stromal cells of breast cancers. Nat Genet *37*, 899-905.

Jolicoeur, F. (2005). Intrauterine breast development and the mammary myoepithelial lineage. J Mammary Gland Biol Neoplasia *10*, 199-210.

Jones, J.L., Shaw, J.A., Pringle, J.H., and Walker, R.A. (2003). Primary breast myoepithelial cells exert an invasion-suppressor effect on breast cancer cells via paracrine down-regulation of MMP expression in fibroblasts and tumour cells. J Pathol *201*, 562-572.

Kuperwasser, C., Chavarria, T., Wu, M., Magrane, G., Gray, J.W., Carey, L., Richardson, A., and Weinberg, R.A. (2004). Reconstruction of functionally normal and malignant human breast tissues in mice. Proc Natl Acad Sci U S A *101*, 4966-4971.

Leo, C., Faber, S., Hentschel, B., Hockel, M., and Horn, L.C. (2006). The status of cyclooxygenase-2 expression in ductal carcinoma in situ lesions and invasive breast cancer correlates to cyclooxygenase-2 expression in normal breast tissue. Ann Diagn Pathol *10*, 327-332.

Lerwill, M.F. (2004). Current practical applications of diagnostic immunohistochemistry in breast pathology. Am J Surg Pathol *28*, 1076-1091.

Lewis, M.T., Ross, S., Strickland, P.A., Sugnet, C.W., Jimenez, E., Scott, M.P., and Daniel, C.W. (1999). Defects in mouse mammary gland development caused by conditional haploinsufficiency of Patched-1. Development *126*, 5181-5193.

Liu, S., Dontu, G., Mantle, I.D., Patel, S., Ahn, N.S., Jackson, K.W., Suri, P., and Wicha, M.S. (2006). Hedgehog signaling and Bmi-1 regulate self-renewal of normal and malignant human mammary stem cells. Cancer Res *66*, 6063-6071.

Liu, S., Dontu, G., and Wicha, M.S. (2005). Mammary stem cells, self-renewal pathways, and carcinogenesis. Breast Cancer Res *7*, 86-95.

Ma, X.J., Salunga, R., Tuggle, J.T., Gaudet, J., Enright, E., McQuary, P., Payette, T., Pistone, M., Stecker, K., Zhang, B.M.*, et al.* (2003). Gene expression profiles of human breast cancer progression. Proc Natl Acad Sci U S A *100*, 5974-5979.

Man, Y.G., Tai, L., Barner, R., Vang, R., Saenger, J.S., Shekitka, K.M., Bratthauer, G.L., Wheeler, D.T., Liang, C.Y., Vinh, T.N., and Strauss, B.L. (2003). Cell clusters overlying focally disrupted mammary myoepithelial cell layers and adjacent cells within the same duct display different immunohistochemical and genetic features: implications for tumor progression and invasion. Breast Cancer Res *5*, R231-241.

Mann, J.R., Backlund, M.G., and DuBois, R.N. (2005). Mechanisms of disease: Inflammatory mediators and cancer prevention. Nat Clin Pract Oncol *2*, 202-210.

McKeon, F. (2004). p63 and the epithelial stem cell: more than status quo? Genes Dev *18*, 465-469.

Miller, F. (2000). Xenograft models of premalignant breast disease. J Mammary Gland Biol Neoplasia *5*, 379-391.

Miller, F.R., Santner, S.J., Tait, L., and Dawson, P.J. (2000). MCF10DCIS.com xenograft model of human comedo ductal carcinoma in situ [letter]. J Natl Cancer Inst *92*, 1185-1186.

Miller, F.R., Soule, H.D., Tait, L., Pauley, R.J., Wolman, S.R., Dawson, P.J., and Heppner, G.H. (1993). Xenograft model of progressive human proliferative breast disease. J Natl Cancer Inst *85*, 1725-1732.

Mishra, L., Shetty, K., Tang, Y., Stuart, A., and Byers, S.W. (2005). The role of TGF-beta and Wnt signaling in gastrointestinal stem cells and cancer. Oncogene *24*, 5775-5789.

Munger, J.S., Huang, X., Kawakatsu, H., Griffiths, M.J., Dalton, S.L., Wu, J., Pittet, J.F., Kaminski, N., Garat, C., Matthay, M.A.*, et al.* (1999). The integrin alpha v beta 6 binds and activates latent TGF beta 1: a mechanism for regulating pulmonary inflammation and fibrosis. Cell *96*, 319-328.

Ney, P.A., Andrews, N.C., Jane, S.M., Safer, B., Purucker, M.E., Weremowicz, S., Morton, C.C., Goff, S.C., Orkin, S.H., and Nienhuis, A.W. (1993). Purification of the human NF-E2 complex: cDNA cloning of the hematopoietic cell-specific subunit and evidence for an associated partner. Mol Cell Biol *13*, 5604-5612.

Peters, B.A., Diaz, L.A., Polyak, K., Meszler, L., Romans, K., Guinan, E.C., Antin, J.H., Myerson, D., Hamilton, S.R., Vogelstein, B.*, et al.* (2005). Contribution of bone marrow-derived endothelial cells to human tumor vasculature. Nat Med *11*, 261-262.

Polyak, K., and Hu, M. (2005). Do myoepithelial cells hold the key for breast tumor progression? J Mammary Gland Biol Neoplasia *10*, 231-247.

Polyak, K., Lee, M.H., Erdjument-Bromage, H., Koff, A., Roberts, J.M., Tempst, P., and Massague, J. (1994). Cloning of p27Kip1, a cyclin-dependent kinase inhibitor and a potential mediator of extracellular antimitogenic signals. Cell *78*, 59-66.

Porter, D., Lahti-Domenici, J., Keshaviah, A., Bae, Y.K., Argani, P., Marks, J., Richardson, A., Cooper, A., Strausberg, R., Riggins, G.J.*, et al.* (2003). Molecular markers in ductal carcinoma in situ of the breast. Mol Cancer Res *1*, 362-375.

Porter, D.A., Krop, I.E., Nasser, S., Sgroi, D., Kaelin, C.M., Marks, J.R., Riggins, G., and Polyak, K. (2001). A SAGE (serial analysis of gene expression) view of breast tumor progression. Cancer Res *61*, 5697-5702.

Radisky, D.C., Levy, D.D., Littlepage, L.E., Liu, H., Nelson, C.M., Fata, J.E., Leake, D., Godden, E.L., Albertson, D.G., Nieto, M.A.*, et al.* (2005). Rac1b and reactive oxygen species mediate MMP-3-induced EMT and genomic instability. Nature *436*, 123-127.

Ronnov-Jessen, L., Petersen, O.W., and Bissell, M.J. (1996). Cellular changes involved in conversion of normal to malignant breast: importance of the stromal reaction. Physiol Rev *76*, 69-125.

Ronnov-Jessen, L., Petersen, O.W., Koteliansky, V.E., and Bissell, M.J. (1995). The origin of the myofibroblasts in breast cancer. Recapitulation of tumor environment in culture unravels diversity and implicates converted fibroblasts and recruited smooth muscle cells. J Clin Invest *95*, 859-873.

Rubin, J.B., Choi, Y., and Segal, R.A. (2002). Cerebellar proteoglycans regulate sonic hedgehog responses during development. Development *129*, 2223-2232.

Santner, S.J., Dawson, P.J., Tait, L., Soule, H.D., Eliason, J., Mohamed, A.N., Wolman, S.R., Heppner, G.H., and Miller, F.R. (2001). Malignant MCF10CA1 cell lines derived from premalignant human breast epithelial MCF10AT cells. Breast Cancer Res Treat *65*, 101-110.

Sato, N., Maehara, N., and Goggins, M. (2004). Gene expression profiling of tumor-stromal interactions between pancreatic cancer cells and stromal fibroblasts. Cancer Res *64*, 6950-6956.

Shay, J.W., Tomlinson, G., Piatyszek, M.A., and Gollahon, L.S. (1995). Spontaneous in vitro immortalization of breast epithelial cells from a patient with Li-Fraumeni syndrome. Mol Cell Biol *15*, 425-432.

Shim, V., Gauthier, M.L., Sudilovsky, D., Mantei, K., Chew, K.L., Moore, D.H., Cha, I., Tlsty, T.D., and Esserman, L.J. (2003). Cyclooxygenase-2 expression is related to nuclear grade in ductal carcinoma in situ and is increased in its normal adjacent epithelium. Cancer Res *63*, 2347-2350.

Simpson, P.T., Reis-Filho, J.S., Gale, T., and Lakhani, S.R. (2005). Molecular evolution of breast cancer. J Pathol *205*, 248-254.

Singh, B., Berry, J.A., Shoher, A., Ramakrishnan, V., and Lucci, A. (2005). COX-2 overexpression increases motility and invasion of breast cancer cells. Int J Oncol *26*, 1393-1399.

Sternlicht, M.D., Lochter, A., Sympson, C.J., Huey, B., Rougier, J.P., Gray, J.W., Pinkel, D., Bissell, M.J., and Werb, Z. (1999). The stromal proteinase MMP3/stromelysin-1 promotes mammary carcinogenesis. Cell *98*, 137-146.

Stingl, J., Eaves, C.J., Kuusk, U., and Emerman, J.T. (1998). Phenotypic and functional characterization in vitro of a multipotent epithelial cell present in the normal adult human breast. Differentiation *63*, 201-213.

Stingl, J., Eaves, C.J., Zandieh, I., and Emerman, J.T. (2001). Characterization of bipotent mammary epithelial progenitor cells in normal adult human breast tissue. Breast Cancer Res Treat *67*, 93-109.

Stingl, J., Raouf, A., Emerman, J.T., and Eaves, C.J. (2005). Epithelial progenitors in the normal human mammary gland. J Mammary Gland Biol Neoplasia *10*, 49-59.

Tait, L., Dawson, P.J., Wolman, S.R., Galea, K., and Miller, F.R. (1996). Multipotent human breast stem cell line MCF10AT. Int J Oncol *9*, 263-267.

Thomasset, N., Lochter, A., Sympson, C.J., Lund, L.R., Williams, D.R., Behrendtsen, O., Werb, Z., and Bissell, M.J. (1998). Expression of autoactivated stromelysin-1 in mammary glands of transgenic mice leads to a reactive stroma during early development. Am J Pathol *153*, 457-467.

Tlsty, T.D., and Hein, P.W. (2001). Know thy neighbor: stromal cells can contribute oncogenic signals. Curr Opin Genet Dev *11*, 54-59.

Waltermann, A., Kartasheva, N.N., and Dobbelstein, M. (2003). Differential regulation of p63 and p73 expression. Oncogene *22*, 5686-5693.

Weinberg, R., and Mihich, E. (2006). Eighteenth annual pezcoller symposium: tumor microenvironment and heterotypic interactions. Cancer Res *66*, 11550-11553.

Yao, J., Weremowicz, S., Feng, B., Gentleman, R.C., Marks, J.R., Gelman, R., Brennan, C., and Polyak, K. (2006). Combined cDNA array comparative genomic hybridization and serial analysis of gene expression analysis of breast tumor progression. Cancer Res *66*, 4065-4078.

Yehiely, F., Moyano, J.V., Evans, J.R., Nielsen, T.O., and Cryns, V.L. (2006). Deconstructing the molecular portrait of basal-like breast cancer. Trends Mol Med *12*, 537-544.

Yokota, T., Yoshimoto, M., Akiyama, F., Sakamoto, G., Kasumi, F., Nakamura, Y., and Emi, M. (1999). Frequent multiplication of chromosomal region 8q24.1 associated with aggressive histologic types of breast cancers. Cancer Lett *139*, 7-13.

Zambruno, G., Marchisio, P.C., Marconi, A., Vaschieri, C., Melchiori, A., Giannetti, A., and De Luca, M. (1995). Transforming growth factor-beta 1 modulates beta 1 and beta 5 integrin receptors and induces the de novo expression of the alpha v beta 6 heterodimer in normal human keratinocytes: implications for wound healing. J Cell Biol *129*, 853-865.

FIGURE LEGENDS

Figure 1. Histologic similarity of MCFDCIS model to human DCIS. A: Comparison of MCFDCIS xenografts and human high-grade comedo DCIS analyzed by hematoxylin-eosin staining (H&E) to depict histology and immunohistochemistry for the expression of SMA, CD10, p63, ITGB6, and basement membrane (BM) marker laminin 5. **B:** Progression of the MCFDCIS xenografts. Histology of the tumors (H&E) and expression of SMA, p63, and ITGB6 were analyzed at the indicated time points after injection. **C:** Immuno-FISH analysis of the time course experiment demonstrates the presence of SMA-positive human myoepithelial cells in DCIS that disappear in invasive tumors. Immunofluorescence using smooth muscle actin antibody (SMA-blue) identifies myoepithelial cells or myofibroblasts. Fluorescently labeled human (green) and mouse (red) Cot1 DNA were used as probes for FISH. Yellow arrows and stars indicate human myoepithelial cells and mouse myofibroblasts, respectively.

Figure 2. Progenitor property of MCFDCIS cells. A: Immunohistochemical analyses of the indicated markers in MCFDCIS cells (*in vitro*) or xenografts (*in vivo*). **B:** Immunocytochemical analysis of CK14 expression in independent single-cell clones of MCFDCIS cells. **C:** Immunoblot analysis of CK14 and MUC1 expression in independent single-cell clones of MCFDCIS cells. **D:** Immunohistochemical analyses of the indicated markers in xenografts derived from the single-cell clones. All clones gave rise to DCIS-like tumors, but clone 7 had a more invasive component. *In vivo,* the expression pattern of all proteins is the same in all clones regardless of their expression *in vitro*.

Figure 3. Molecular similarity of MCFDCIS model to human DCIS. A: Semi-quantitative RT-PCR analysis of the expression of cell type-specific markers, and mediators of TGFβ1 and hedgehog (Hh) signaling in MUC1+ and ITGB6+ cells purified from DCIS xenografts. Myoepithelial markers are only detected in ITGB6+ cells. ITGB6+ cells also show higher levels of certain genes involved in TGFβ1 and Hh signaling. **B:** Cluster analysis of the indicated SAGE libraries to delineate similarities of MUC1+ and

ITGB6+ cells to human breast epithelial and myoepithelial cells, respectively. **C:** Gene ontology categories enriched in ITGB6+ myoepithelial and MUC1+ luminal epithelial cells. Scores >1.3 corresponds to $p < 0.05$. **D:** Relative expression level of MMP14 in bulk DCIS (cadmium yellow) and invasive ductal carcinoma (crimson), and in epithelial (red) and myoepithelial (green) cells purified from normal breast tissue, *in situ* and invasive carcinomas. **E:** Relative expression level of MMP14 in MUC1+ (red) and ITGB6+(green) cells.

Figure 4. The effect of non-epithelial cells on MCFDCIS xenograft growth and histology. A: The effect of co-injection of different cells on tumor weight. Normal myoepithelial cells (HME) statistically significantly suppressed tumor weight ($p=0.04$), fibroblasts from normal breast (PBS) had no effect ($P=0.61$), and fibroblasts from breast tumors (PBTS) and rheumatoid arthritis synovium (RASF) increased tumor weight ($p=0.08$ and $p=0.15$, respectively). **B:** Histological and immunohistochemical analyses of MCFDCIS xenografts from co-injection experiments. MCFDCIS cells injected alone or co-injected with normal myoepithelial cells form DCIS-like tumors, while co-injection of any fibroblasts results in invasive tumors. In DCIS-like tumors, the expression of p63 and ITGB6 is limited to a layer of cells with myoepithelial features, while in invasive tumors, a subset of epithelial cells are p63 and ITGB6 positive. SMA is detected in myoepithelial cells (only in DCIS-like tumors) and in myofibroblasts. The number of cells positive for the MIB1 proliferation marker correlates with overall tumor size and weight. **C:** Immuno-FISH using pan-cytokeratin antibody (panCK-blue) identifies epithelial cells. The overlay demonstrates the human origin of cytokeratin positive epithelial cells and the mouse origin of stromal cells. **D:** Immuno-FISH using smooth muscle actin antibody (SMA-blue) identifies myoepithelial cells or myofibroblasts. The overlay demonstrates the human origin of SMA-positive myoepithelial cells (yellow arrows) in DCIS structures and the mouse origin of SMA-positive myofibroblasts (yellow stars). **E-F**: The dominant effect of normal myoepithelial cells on tumor weight (**E**) and histology (**F**). Normal myoepithelial cells overcome the tumor weight and progression-enhancing effects of fibroblasts, since

tumors resulting from the injection of MCFDCIS cells together with PBS+HME, PBTS+HME, and RASF+HME are significantly smaller (PBS: p=0.11, PBTS: p=0.09, and RASF: p=0.0007) and have DCIS histology compared to xenografts initiated from MCFDCIS cells co-injected with fibroblasts (PBS, PBTS, or RASF). **G:** The reversibility of the effect of fibroblasts on tumor phenotype. Tumors were removed and analyzed 22 days after injection, at which time tumors from MCFDCIS cells injected alone (-) or co-injected with myoepithelial cells (HME) all form DCIS, while co-injection of breast fibroblasts (PBS or PBTS) results in invasive tumors (Original day 22). Re-injection of cells isolated from these tumors resulted in DCIS-like xenografts (Reinjected day 22).

Figure 5. COX2 as a mediator of epithelial-stromal cell interactions. A: Immunohistochemical analysis of COX2 expression in MCFDCIS xenografts. Low expression is detected in MCFDCIS cells injected alone (-) or co-injected with normal myoepithelial cells (HME), while co-injection of any fibroblasts upregulates COX2 in tumor epithelial cells. **B:** qPCR analysis of human-specific *PTGS2* (COX2), *MMP14*, *VEGFA*, and *VEGFC* gene expression in MCFDCIS xenografts. Decreased and increased expression of these genes is detected in MCFDCIS cells co-injected with normal myoepithelial cells (HME) and fibroblasts (PBS, PBTS, or RASF), respectively. **C-D:** The effect of a COX2 inhibitor (celecoxib) on the weight (**C**) and histology (**D**) of MCFDCIS xenografts derived from cells injected alone (-) or co-injected with RASF on control or celecoxib-containing diets. Xenografts from MCFDCIS cells alone (-) have DCIS histology and low COX2 expression, regardless of diet. Tumors from MCFDCIS cells co-injected with RASF show an invasive phenotype and high COX2 levels in the control diet group. Celecoxib completely abolished the tumor growth-stimulating effects of RASF (p=0.0001), partially inhibited the progression to invasive tumors, and decreased COX2 protein levels. No significant difference in cell proliferation (MIB1) is detected following celecoxib treatment.

Figure 6. Pathways regulating *in situ* to invasive carcinoma progression. A: Immunoblot analysis of TGFβ1-treated MCFDCIS cells in attached or suspension culture. Integrin β6, laminin 5, and vimentin are increased following TGFβ1 treatment regardless of ECM contact. p63 is not affected by TGFβ1, but it is downregulated in suspension. **B:** Immunoblot analysis of MCFDCIS cells infected with control (pBabe), ΔNp63α, and TAp63γ-overexpressing retroviruses. ΔNp63α overexpression increases integrin β6, laminin 5 and vimentin levels. **C:** p63 expression in xenografts derived from vector control (pBabe) and ΔNp63α overexpressing MCFDCIS cells. Despite its widespread overexpression *in vitro*, in xenografts only the myoepithelial cells are positive for p63. **D:** Hypothetical model summarizing our results and explaining *in situ* to invasive carcinoma progression. The MCFDCIS progenitor cells can give rise to myoepithelial and luminal epithelial cells. Myoepithelial cells are necessary for the formation of DCIS, and their differentiation is negatively and positively regulated by stromal fibroblasts and normal myoepithelial cells, respectively, presumably through ECM remodeling. Basement membrane (BM) regulates the myoepithelial phenotype via its influence on p63 expression. At the same time, p63 regulates ECM components and contact, forming a positive feedback loop. The augmented TGFβ1 signaling in myoepithelial cells also modulates cell-ECM interaction. In contrast to the role of normal myoepithelial cells in BM synthesis and maintenance, DCIS-associated myoepithelial cells express high levels of MMP14, leading to gradual degradation of BM. Thus, the balance between BM deposition and deconstruction is the determinant of the *in situ* to invasive transition.

Table 1. Similarity of MUC1+ and ITGB6+ cells to breast epithelial and myoepithelial cells purified from primary human tissue samples. Detailed description of SAGE libraries and analysis of SAGE data are included in the Supplemental data section. Genes were selected based on the following criteria: (1) statistically significant ($p<0.05$) difference between ITGB6+ and MUC1+ libraries; (2) statistically significant ($p<0.05$) difference between human MYOEP and EPI groups based on t-test or Wilcox test (for rows A and B), or ratio of DMYOEP/NMYOEP $\geq$ 10-fold (for row C); (3) ratio of ITGB6+/MUC1+ and MYOEP/EPI are in the same direction; (4) ratio of both ITGB6+/MUC1+ and MYOEP/EPI are $\geq$ 2-fold; and (5) tag count $\geq$10 in at least one of the primary human tissue libraries. Normalized tag counts, Unigene ID, gene symbol, gene description, and cellular localization (LOC) are listed. Abbreviation: N-normal, D-ductal carcinoma *in situ*, I-invasive ductal carcinoma, PM-plasma membrane, EC-extracellular, IC-intracellular, and NU-nuclear. Genes related to TGFβ1 signaling are highlighted in yellow. Rows "A" and "B" denote genes high in ITGB6+ and MYOEP and MUC1+ and EPI cells, respectively, and row "C" represents genes high in ITGB6+ and D-MYOEP cells.

			MYOEP					EPI											
	ITGB6+	MUC1+	N-MYOEP-1	N-MYOEP-2	N-MYOEP-4	D-MYOEP-6	D-MYOEP-7	N-EPI-1	N-EPI-2	D-EPI-2	D-EPI-3	D-EPI-6	D-EPI-7	I-EPI-7	I-EPI-8	I-EPI-9	UNIGENE	GENE SYMBOL	GENE DESCRIPTION	LOC
A	63	1	59	17	11	597	173	2	0	2	7	25	7	10	59	17	111779	SPARC	Secreted protein, acidic, cysteine-rich (osteonectin)	EC
	90	4	112	136	263	260	204	53	14	8	17	56	64	14	8	5	534330	MT2A	Metallothionein 2A	EC
	54	3	91	33	54	12	10	33	20	3	0	3	1	5	0	0	591484	LAMC2	Laminin, gamma 2	EC
	24	1	114	45	149	36	58	0	6	5	0	8	4	3	15	3	632099	TAGLN	Transgelin	IC
	24	1	14	41	39	16	17	2	0	0	3	3	1	5	0	0	300772	TPM2	Tropomyosin 2 (beta)	IC
	20	1	9	20	7	6	15	0	0	0	2	1	0	0	0	0	508716	COL4A2	Collagen, type IV, alpha 2	EC
	13	0	45	31	13	26	38	2	2	6	3	5	3	5	8	20	504687	MYL9	Myosin, light polypeptide 9, regulatory	IC
	121	13	7	48	26	91	56	4	2	3	16	4	2	7	23	5	110675	TOMM40	Translocase of outer mitochondrial membrane 40 homolog	IC
	12	0	16	5	5	20	31	0	0	0	0	1	0	0	0	0	590970	AXL	AXL receptor tyrosine kinase	PM
	12	1	23	42	17	59	60	18	0	0	9	5	2	3	11	0	503911	NNMT	Nicotinamide N-methyltransferase	IC
	23	3	58	53	28	106	162	0	0	8	21	10	7	4	17	23	591346	CTGF	Connective tissue growth factor	EC
	9	0	26	39	18	96	37	0	6	2	3	8	7	7	8	2	62886	SPARCL1	SPARC-like 1 (mast9, hevin)	EC
	8	0	12	6	0	31	17	0	2	0	0	5	0	0	0	0	17441	COL4A1	Collagen, type IV, alpha 1	EC
	8	0	12	8	24	5	23	6	4	3	3	23	9	0	3	2	474833	CSNK1E	Casein kinase 1, epsilon	IC
	8	0	10	16	3	14	4	0	0	0	3	0	1	1	3	0	111779	SPARC	Secreted protein, acidic, cysteine-rich (osteonectin)	EC
	24	6	37	47	29	76	13	18	8	14	5	5	8	16	2	26	370771	CDKN1A	Cyclin-dependent kinase inhibitor 1A (p21, Cip1)	NU
	42	10	87	34	18	11	6	16	16	5	5	4	10	5	6	5	133892	TPM1	Tropomyosin 1 (alpha)	IC
	17	4	3	14	7	5	8	0	2	2	2	4	0	1	5	0	298654	DUSP6	Dual specificity phosphatase 6	IC
	82	22	66	122	159	44	29	16	26	5	3	4	1	1	3	2	433845	KRT5	Keratin 5	IC
	107	37	38	36	101	102	121	4	8	3	10	15	6	7	20	15	533317	VIM	Vimentin	IC
	28	10	19	14	9	31	23	2	8	3	3	8	9	34	0	5	223678	JMJD3	Jumonji domain containing 3	
B	47	99	2	23	11	7	4	39	53	139	14	22	76	33	56	21	301350	FXYD3	FXYD domain containing ion transport regulator 3	PM
	24	55	2	78	5	0	17	47	154	106	35	118	1090	347	51	120	520943	NCF1	Neutrophil cytosolic factor 1	PM
	16	37	3	5	4	2	0	2	12	14	17	0	9	7	5	5	346868	EBNA1BP2	EBNA1 binding protein 2	NU
	11	32	3	22	12	2	0	31	26	88	7	19	43	16	12	8	464210	SYNGR2	Synaptogyrin 2	PM
	7	21	0	2	0	0	0	2	6	36	0	12	15	5	21	5	485158	SPDEF	SAM pointed domain containing ets transcription factor	NU
	7	21	0	9	5	0	0	33	10	18	5	7	10	16	3	9	194385	STAP2	Signal-transducing adaptor protein-2	IC
	13	59	0	42	4	1	2	62	168	228	5	167	105	68	11	174	375108	CD24	CD24 molecule	PM
	0	7	0	5	0	0	0	4	6	12	2	10	19	7	14	3	642705	KIAA1324	KIAA1324	
	0	9	2	5	5	0	4	6	18	11	7	16	19	1	3	11	542050	TACSTD1	Tumor-associated calcium signal transducer 1	PM
	0	9	37	20	14	16	10	88	51	207	33	30	109	68	47	27	437638	XBP1	X-box binding protein 1	NU
	1	10	5	2	0	1	4	6	18	8	2	4	10	4	11	18	130413	TM9SF2	Transmembrane 9 superfamily member 2	IC
	30	275	0	2	1	0	0	12	14	23	17	1	1	3	60	8	46452	SCGB2A2	Secretoglobin, family 2A, member 2	EC
	0	21	3	3	4	2	0	10	6	27	5	15	15	10	6	14	201083	MAL2	Mal, T-cell differentiation protein 2	PM
	1	61	0	2	0	0	0	8	4	2	2	3	6	10	12	2	105887	LOC124220	Similar to common salivary protein 1	EC
C	15	1	5	8	5	55	77	14	22	45	0	11	4	3	3	12	448588	NGFRAP1	Nerve growth factor receptor associated protein 1	NU
	13	0	0	2	0	15	48	0	0	0	2	4	0	0	0	0	821	BGN	Biglycan	EC
	9	0	3	5	1	45	58	2	2	6	9	29	8	15	8	20	522584	TMSB4X	Thymosin, beta 4, X-linked	IC
	40	9	2	2	1	21	19	0	0	2	5	1	0	0	6	0	7835	MRC2	Mannose receptor, C type 2	PM
	17	4	0	6	3	69	27	0	4	0	0	4	3	4	8	5	529053	C3	Complement component 3	EC
	42	13	0	5	4	20	79	6	0	6	2	7	22	8	5	18	289019	LTBP3	Latent transforming growth factor beta binding protein 3	EC

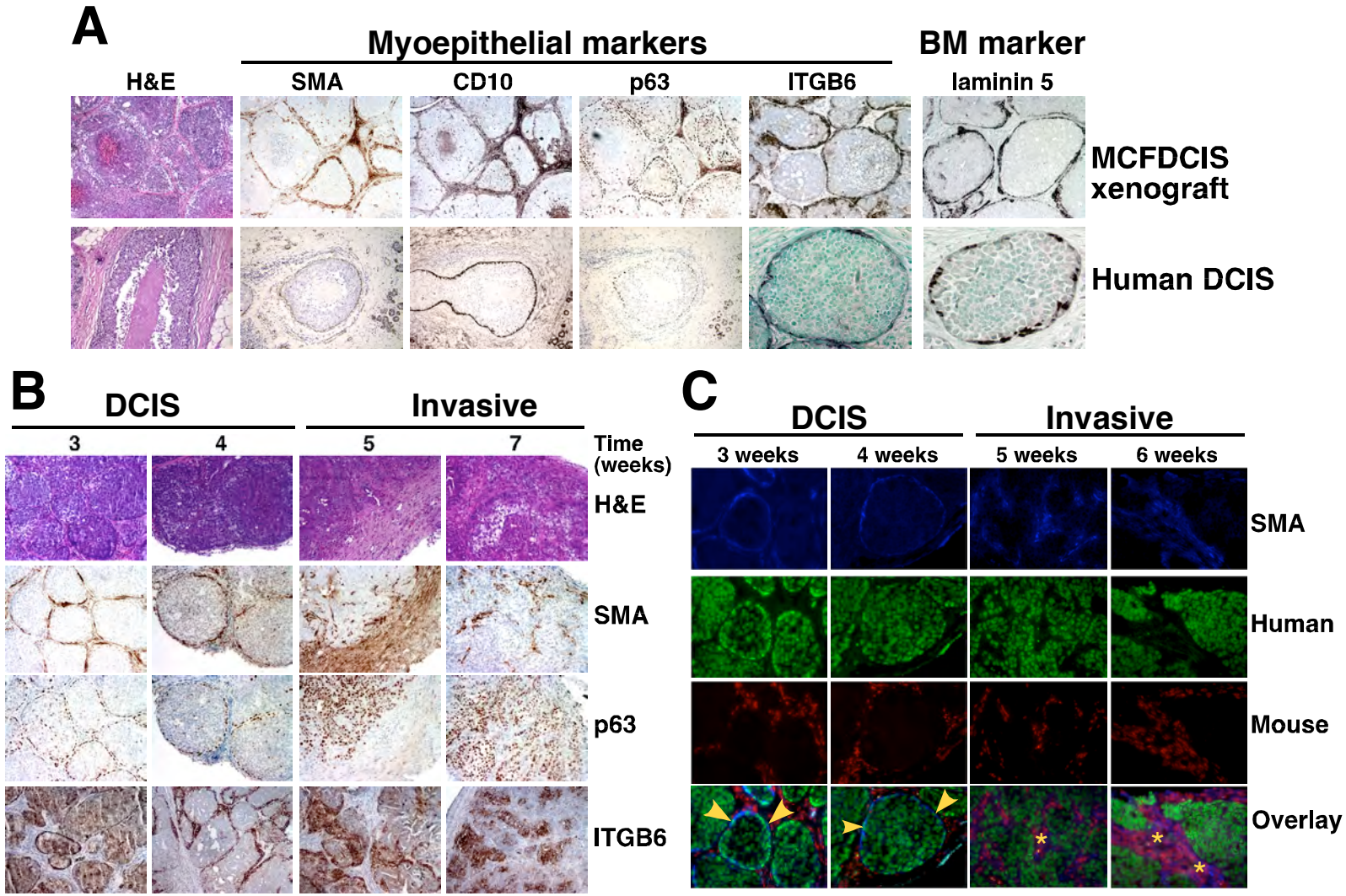
A
Myoepithelial markers
BM marker
H&E
SMA
CD10
p63
ITGB6
laminin 5
MCFDCIS xenograft
Human DCIS
B
DCIS
Invasive
3
4
5
7
Time (weeks)
H&E
SMA
p63
ITGB6
C
DCIS
Invasive
3 weeks
4 weeks
5 weeks
6 weeks
SMA
Human
Mouse
Overlay

FIGURE 1

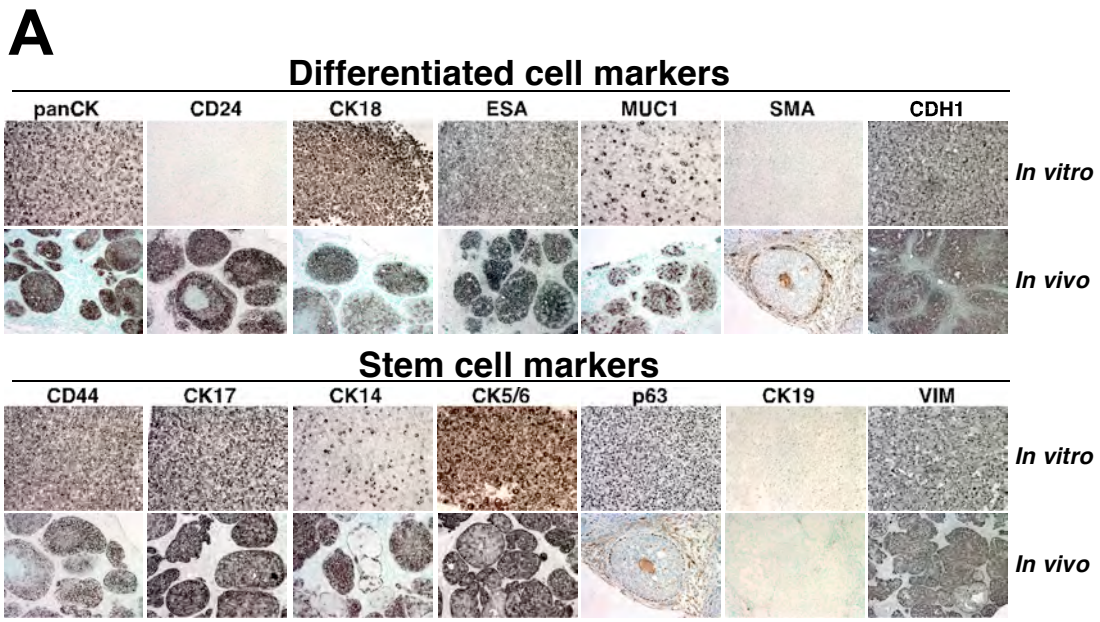
A
Differentiated cell markers
panCK
CD24
CK18
ESA
MUC1
SMA
CDH1
In vitro
In vivo
Stem cell markers
CD44
CK17
CK14
CK5/6
p63
CK19
VIM
In vitro
In vivo

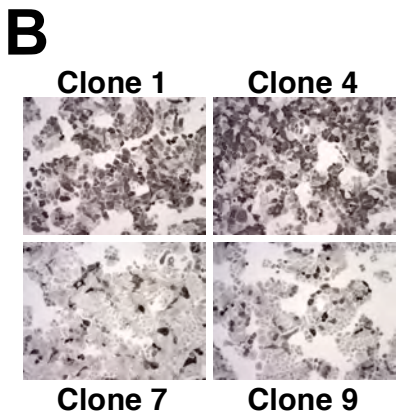
B
Clone 1
Clone 4
Clone 7
Clone 9

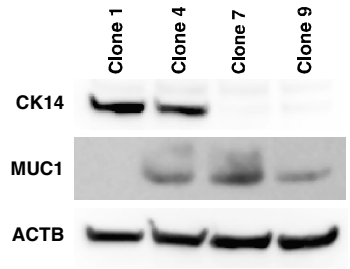
C
Clone 1
Clone 4
Clone 7
Clone 9
CK14
MUC1
ACTB

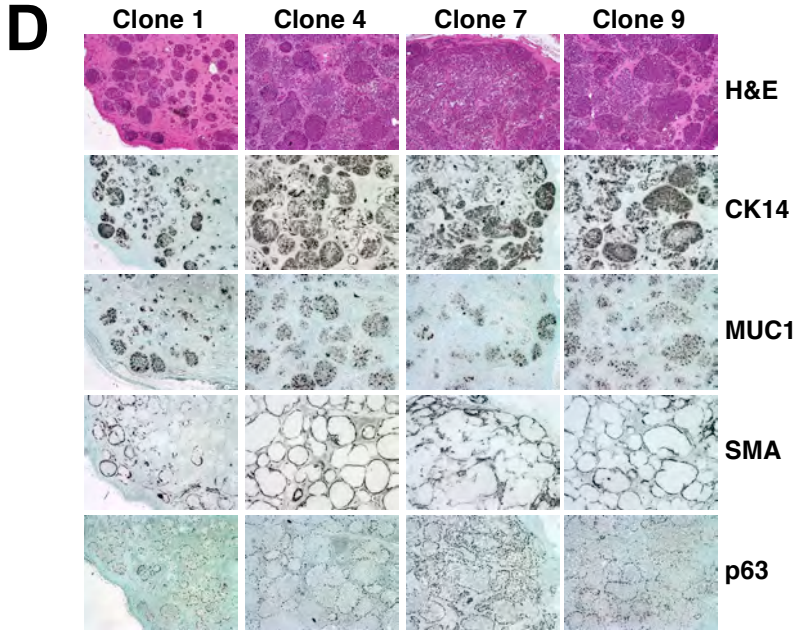
D
Clone 1
Clone 4
Clone 7
Clone 9
H&E
CK14
MUC1
SMA
p63

FIGURE 2

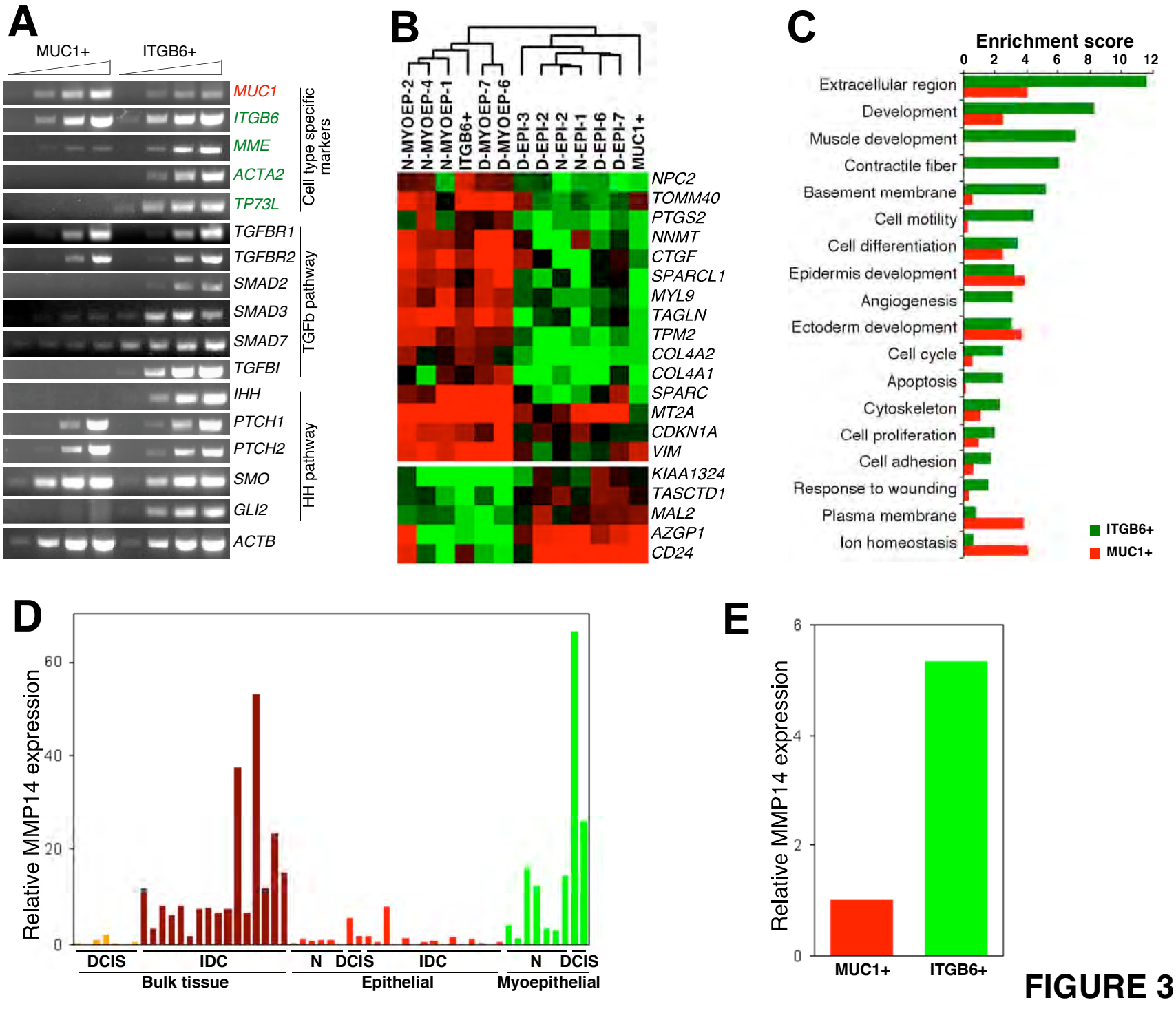
A
MUC1+
ITGB6+
MUC1
ITGB6
MME
ACTA2
TP73L
TGFBR1
TGFBR2
SMAD2
SMAD3
SMAD7
TGFBI
IHH
PTCH1
PTCH2
SMO
GLI2
ACTB
Cell type specific markers
TGFb pathway
HH pathway
B
N-MYOEP-2
N-MYOEP-4
N-MYOEP-1
ITGB6+
D-MYOEP-7
D-MYOEP-6
D-EPI-3
D-EPI-2
N-EPI-2
N-EPI-1
D-EPI-6
D-EPI-7
MUC1+
NPC2
TOMM40
PTGS2
NNMT
CTGF
SPARCL1
MYL9
TAGLN
TPM2
COL4A2
COL4A1
SPARC
MT2A
CDKN1A
VIM
KIAA1324
TASCTD1
MAL2
AZGP1
CD24
C
Enrichment score
0 2 4 6 8 10 12
Extracellular region
Development
Muscle development
Contractile fiber
Basement membrane
Cell motility
Cell differentiation
Epidermis development
Angiogenesis
Ectoderm development
Cell cycle
Apoptosis
Cytoskeleton
Cell proliferation
Cell adhesion
Response to wounding
Plasma membrane
Ion homeostasis
ITGB6+
MUC1+
D
Relative MMP14 expression
0
20
40
60
DCIS
IDC
N
DCIS
IDC
N
DCIS
Bulk tissue
Epithelial
Myoepithelial
E
Relative MMP14 expression
0
2
4
6
MUC1+
ITGB6+

FIGURE 3

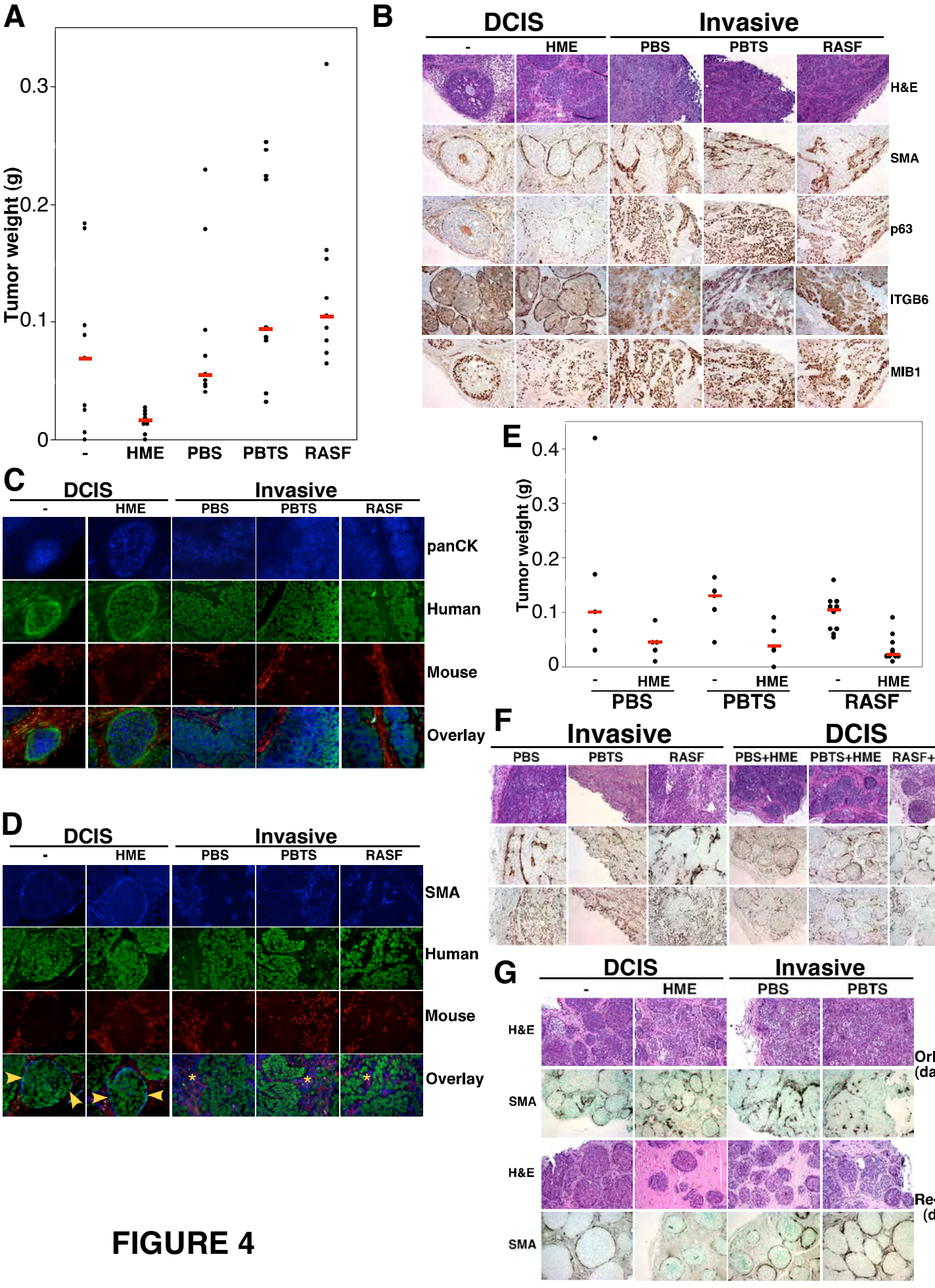
A
Tumor weight (g)
0.3
0.2
0.1
0
-
HME
PBS
PBTS
RASF
B
DCIS
Invasive
-
HME
PBS
PBTS
RASF
H&E
SMA
p63
ITGB6
MIB1
C
DCIS
Invasive
-
HME
PBS
PBTS
RASF
panCK
Human
Mouse
Overlay
D
DCIS
Invasive
-
HME
PBS
PBTS
RASF
SMA
Human
Mouse
Overlay
E
Tumor weight (g)
0.4
0.3
0.2
0.1
0
-
HME
-
HME
-
HME
PBS
PBTS
RASF
F
Invasive
DCIS
PBS
PBTS
RASF
PBS+HME
PBTS+HME
RASF+HME
H&E
SMA
p63
G
DCIS
Invasive
-
HME
PBS
PBTS
H&E
SMA
Orlginal
(day 22)
H&E
SMA
Re-injected
(day 22)

FIGURE 4

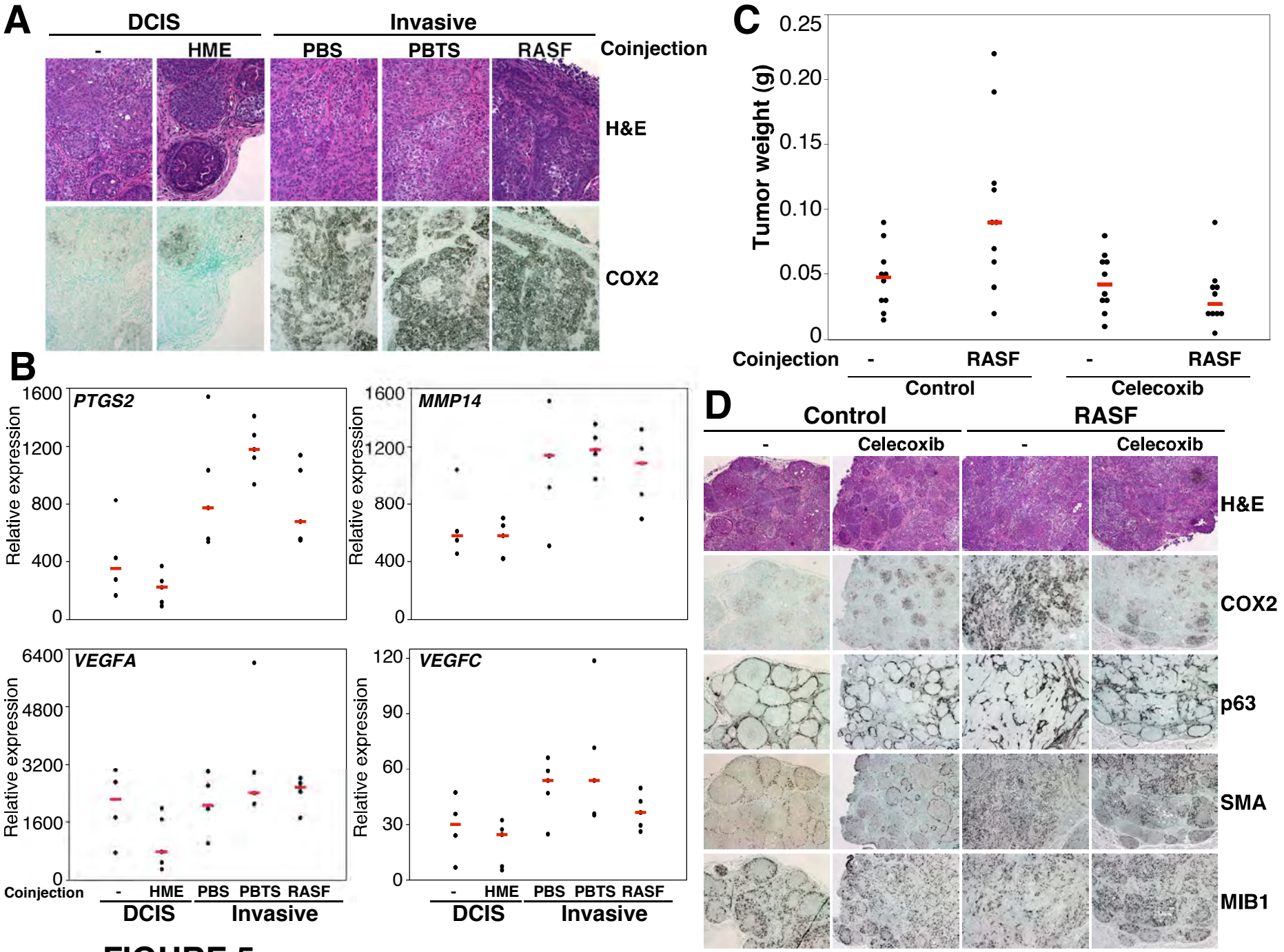
A
DCIS
Invasive
-
HME
PBS
PBTS
RASF
Coinjection
H&E
COX2
B
PTGS2
MMP14
VEGFA
VEGFC
Relative expression
1600
1200
800
400
0
6400
4800
3200
1600
120
90
60
30
Coinjection
- HME PBS PBTS RASF
DCIS
Invasive
C
Tumor weight (g)
0.25
0.20
0.15
0.10
0.05
0
Coinjection
- RASF - RASF
Control
Celecoxib
D
Control
RASF
- Celecoxib - Celecoxib
H&E
COX2
p63
SMA
MIB1

FIGURE 5

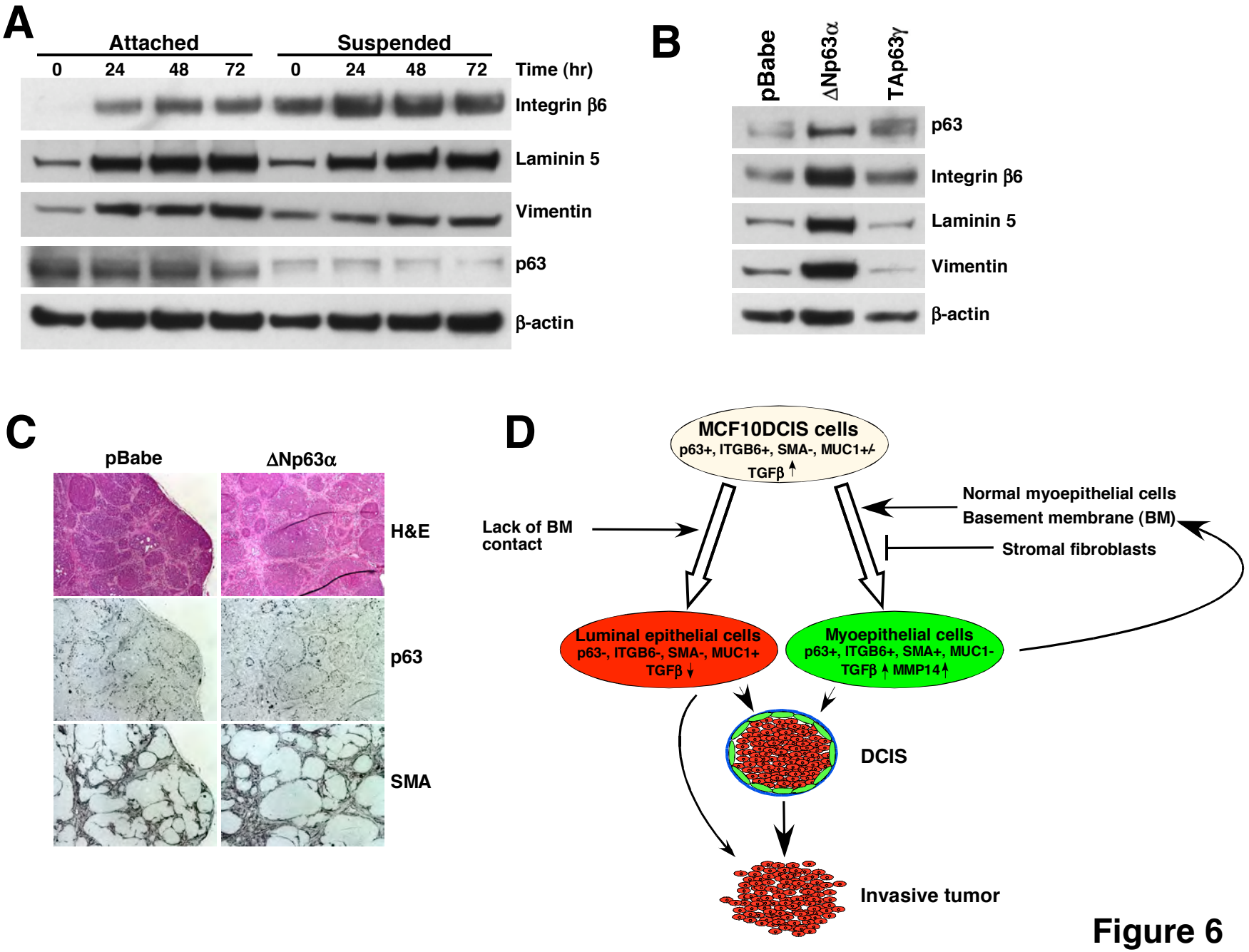
A
Attached
Suspended
0
24
48
72
0
24
48
72
Time (hr)
Integrin β6
Laminin 5
Vimentin
p63
β-actin
B
pBabe
ΔNp63α
TAp63γ
p63
Integrin β6
Laminin 5
Vimentin
β-actin
C
pBabe
ΔNp63α
H&E
p63
SMA
D
MCF10DCIS cells
p63+, ITGB6+, SMA-, MUC1+/-
TGFβ ↑
Lack of BM contact
Normal myoepithelial cells
Basement membrane (BM)
Stromal fibroblasts
Luminal epithelial cells
p63-, ITGB6-, SMA-, MUC1+
TGFβ ↓
Myoepithelial cells
p63+, ITGB6+, SMA+, MUC1-
TGFβ ↑ MMP14 ↑
DCIS
Invasive tumor

Figure 6

SUPPLEMENTAL DATA

Supplemental Table 1. List of antibodies used. Antigen, antibody clone name, source, catalogue number (cat#), species, and application are listed. Abbreviations: FACS - Fluorescence-activated cell sorting, IB-Immunoblot, ICC-Immunocytochemistry, IHC-Immunohistochemistry, I-FISH-Immunofluorescence combined with fluorescence in situ hybridization (FISH). Secondary antibodies were purchased from PIERCE (Rockford, IL) or Jackson ImmunoResearch Laboratories (West Grove, PA)

Antigen	Clone name	Source	Cat #	Species	Application
CD10	56C6	Ventana Medical Systems, Inc	790-2923	mouse	IHC
CD10-RPE	SS2/36	DAKO	R0848	mouse	FACS
CD24	ML5	BD Biosciences	555426	mouse	IHC
CD24-FITC	ML5	BD Biosciences	555427	mouse	FACS
CD44	515	BD Biosciences	550988	mouse	IHC
CD44	156-3C11	NeoMarkers	MS-668-P1	mouse	IHC
CD44-PE	G44-26	BD Biosciences	555479	mouse	FACS
CD49f-PE	GoH3	BD Biosciences	555736	rat	FACS
Cox2		Cayman Chemical	160126	rabbit	IHC
Cox2	CX229	Cayman Chemical	160112	mouse	IHC
Cytokeratin 14	LL002	Novocastra Laboratories	NCL-L-LL002	mouse	IHC, ICC, IB
Cytokeratin 17	E3	DAKO	M7046	mouse	IHC
Cytokeratin 18	C51	Novocastra Laboratories	NCL-C51	mouse	IHC
Cytokeratin 19	RCK108	DAKO	M0888	mouse	IHC
Cytokeratin 5/6	D5/16 B4	DAKO	M7237	mouse	IHC
E-Cadherin	36	BD Biosciences	610181	mouse	IHC
ESA	B302 (323/A3)	Biomeda	V7018	mouse	IHC
ESA-FITC	B29.1 (VU-ID9)	Biomeda	FM010	mouse	FACS
Integrin β6	6.2A1	Dr. Shelia Violette (Biogen Idec, Inc., Cambridge, MA)		mouse	IHC, IB
Integrin β6	6.3G9	Dr. Shelia Violette (Biogen Idec, Inc., Cambridge, MA)		mouse	FACS, purification
Integrin β6	ch2A1	Dr. Shelia Violette (Biogen Idec, Inc., Cambridge, MA)		human	IHC
Ki-67 antigen	MIB1	DAKO	M7240	mouse	IHC
Ki-67 antigen		Vector Laboratories	VP-K451	rabbit	IHC
Laminin 5	9LN5	Dr. William Brunken (Tufts University, Boston, MA)		rabbit	IHC, IB
Muc1	CT2	Dr. Donald Kufe (Dana Farber Cancer Institute, Boston, MA)		hamster	IB
Muc1	DF3	Dr. Donald Kufe (Dana Farber Cancer Institute, Boston, MA)		mouse	IHC, FACS, purification
p63	4A4	Calbiochem	OP132	mouse	IHC, IB
p63	4A4	Chemicon	MAB4135	mouse	IHC
Pan Cytokeratin	AE1/AE3	DAKO	M3515	mouse	IHC, I-FISH
Smooth muscle actin	1A4	DAKO	M0851	mouse	IHC, I-FISH
Vimentin	V9	DAKO	M0725	mouse	IHC, IB
beta-actin	AC-74	Sigma	A2228	mouse	IB

Cluster analysis of SAGE libraries

Differentially expressed tags ($P < 0.05$) between ITGB6+ and MUC1+ SAGE libraries from MCFDCIS xenografts were generated by Poisson analysis (available at http://genome.dfci.harvard.edu/sager/) (Cai et al., 2004). Normalized tag counts per 50,000 from these two libraries were combined with those from human breast epithelial and myoepithelial libraries (N-EPI-1, N-EPI-2, N-MYOEP-1, N-MYOEP-2, N-MYOEP-4, D-EPI-2, D-EPI-3, D-EPI-6, D-EPI-7, D-MYOEP-6, D-MYOEP-7. Tags were further filtered to have a maximum count from all libraries above 10 per 50,000 and to have a >1.5 fold difference between ITGB6 and MUC1 libraries. Filtered data were log transformed and clustered (hierarchical, complete linkage) using the Cluster and TreeView software (Eisen et al., 1998). Color settings were adjusted to set tag count 4 per 50,000 as black. Tag counts below 4 were green and above 4 were red.

Supplemental Figure 1. Characterization of xenografts derived from invasive breast cancer cell lines. Histological and immunohistochemical analyses of the indicated xenografts derived from cell lines injected alone (-) or co-injected with normal myoepithelial cells (+HME). No DCIS histology and myoepithelial cell layer was detected in any of these tumors. SMA (smooth muscle actin) positive cells are mouse myofibroblasts and endothelial cells.

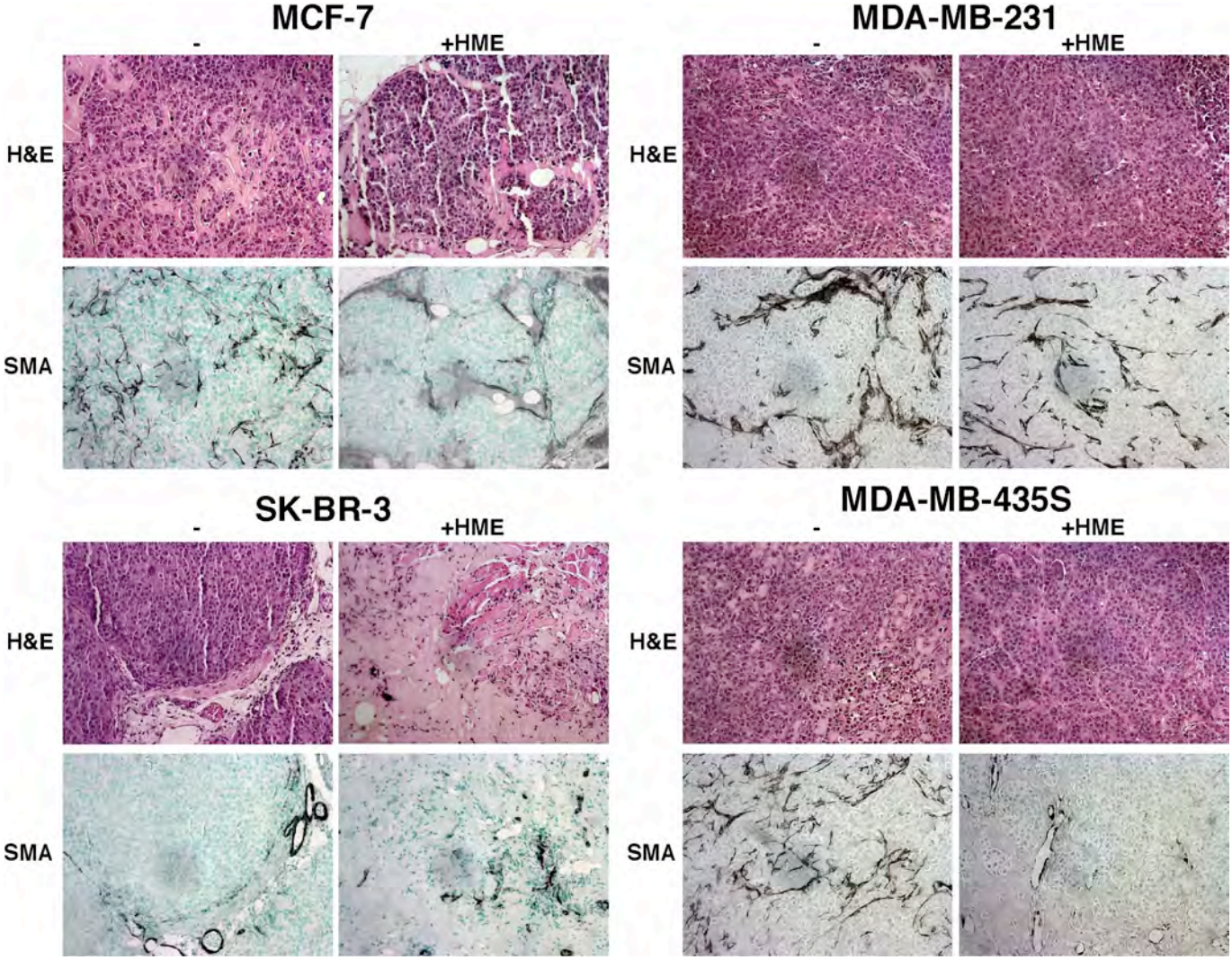

Supplemental Figure 2. Confirming the human origin of cytokeratin positive cells in MCFDCIS xenografts. Immuno-FISH analysis of the time course experiment demonstrates that cytokeratin (CTK) positive cells (blue cytoplasm) are of human origin.

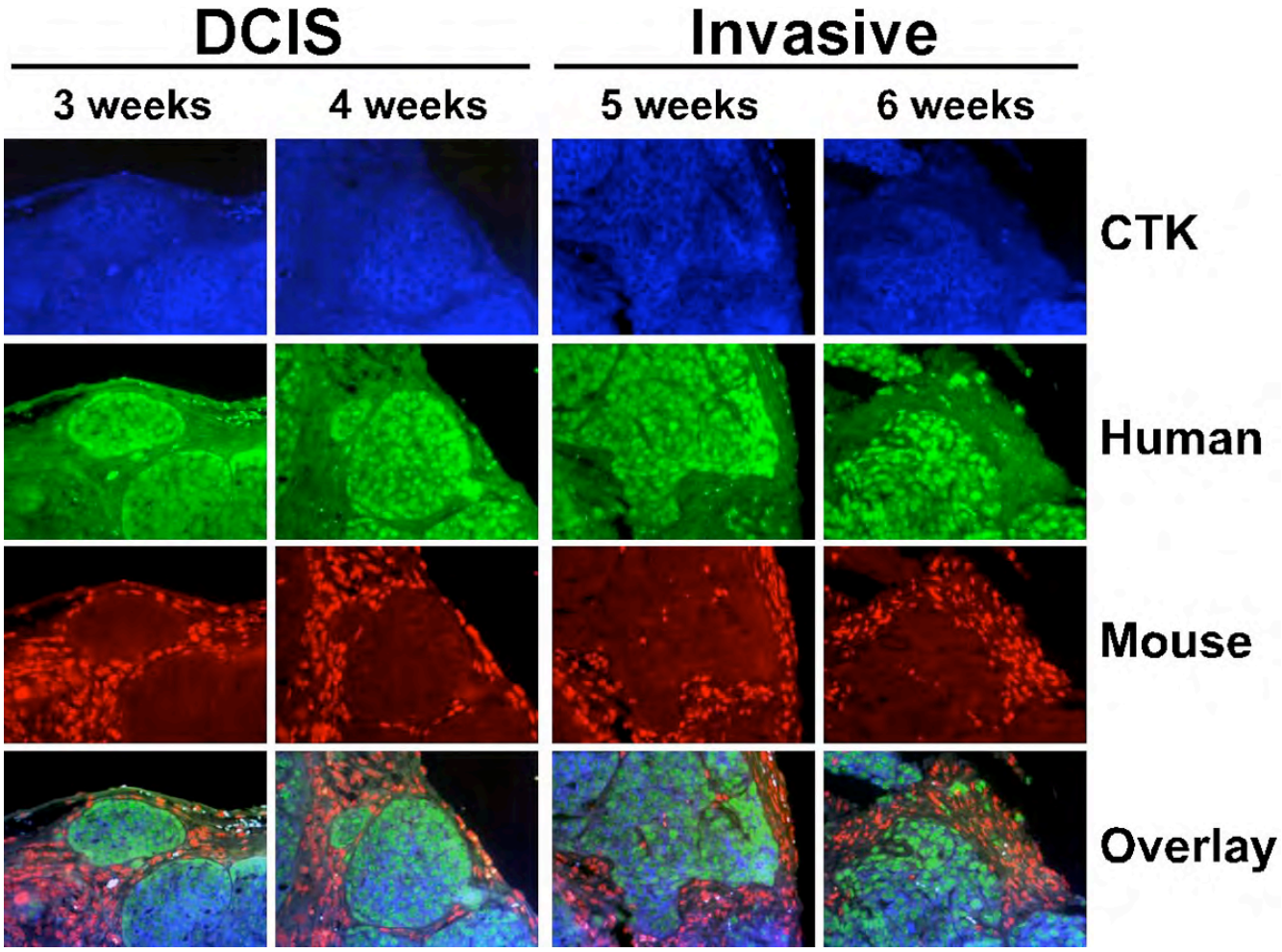

Supplemental Figure 3. Analysis of MCFDCIS cell heterogeneity. A: FACS analysis of cultured cells for the indicated cell surface markers. With the exception of MUC1 the cells are homogenously positive (ITGA6, ESA, ITGB6, and CD44) or negative (CD10 and CD24) for the proteins analyzed. The expression of ITGB6 is further increased following TGFβ1 treatment. **B:** FACS sorting for MUC1+ and MUC1- cells and histology of xenografts resulting from them.

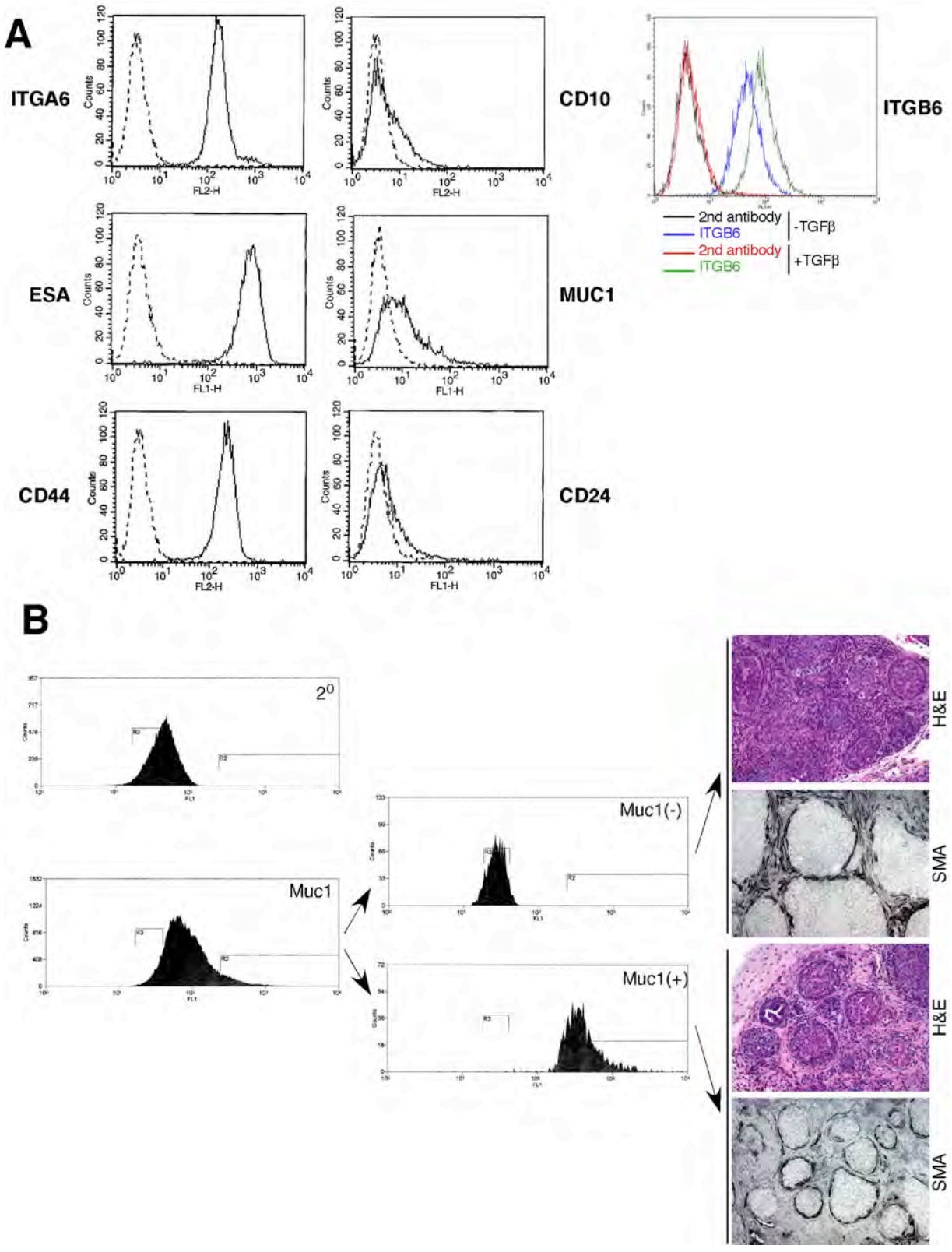

Supplemental Figure 4. Analysis of genetic changes in MCF10A series cells and MCFDCIS derived xenografts. A: SNP array analysis of the indicated cells and xenografts for copy number changes. Copy number gain of 8q24, including *MYC,* and homozygous deletion of *CDKN2A* at 9p21 are indicated. **B:** FISH confirmation of 8q24 copy number gain and insertion to 10q22. Left: *MYC* probe (red) gave three hybridization signals, two on chromosome 8 (green) and one on chromosome 10 (aqua). Right: *MYC* break apart probe (5' red and 3' green) shows two intact copies (yellow fused signal including both 5' and 3' portions) on chromosome 8 (aqua) while the signal on chromosome 10 contains only the 5' portion of the probe (red). **C:** SNP array analysis of the indicated cells and xenografts. An inferred LOH map including all chromosomes indicates that, with the exception of two tumors, all samples are genetically identical to the MCFDCIS cells. Blue and yellow colors indicate LOH and retention of both alleles, respectively.

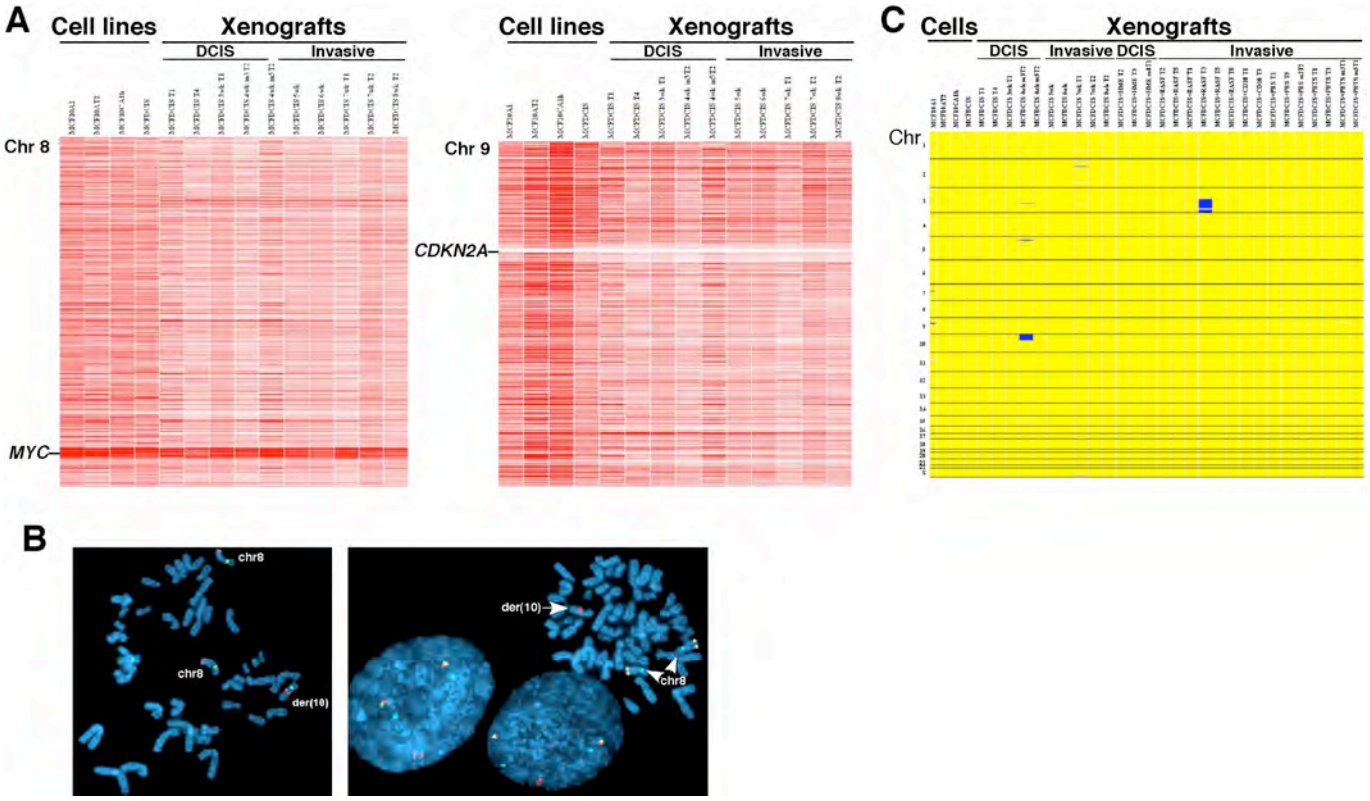

Supplemental Excel Spreadsheet 1. Comparison of SAGE tags that are statistically significantly differentially expressed between ITGB6+ and MUC1+ cells to SAGE libraries prepared from human breast myoepithelial and epithelial cells. All SAGE libraries were normalized to total tag count of 100,000. Tags only present in ITGB6+ or MUC1+ cells from MCFDCIS xenografts and in none of the libraries prepared from primary human tissue were removed. Tags statistically significantly differentially ($p<0.05$) expressed between ITGB6+ and Muc1+ cells were linked to "MYOEP" (CD10+ myoepithelial cells purified from normal breast tissue or DCIS) and "EPI" (BerEP4+ epithelial cells purified from normal or cancerous breast tissue) samples. Two-tailed Student's t-test (T-test) and Wilcox Rank Sum test (Wilcox test) were performed between the "MYOEP" and "EPI" groups, and the ratio of the mean of "MYOEP" and "EPI" groups was calculated (Ratio MYOEP/EPI). If the ratio of ITGB6+/MUC1+ and MYOEP/EPI are in the same and opposite directions then the tag is labeled as "+" and "-", respectively (Direction). To select for DMYOEP specific genes, the ratio of the mean of "DMYOEP" and "NMYOEP" groups was also calculated (Ratio D/N). Tag sequence, normalized tag counts, p value for the difference between ITGB6+ and MUC1+ libraries, T-test, Wilcox test, Mean MYOEP, Mean EPI, Ratio MYOEP/EPI, Direction, Mean DMYOEP, MEAN NMYOEP, Ratio D/N, UniGene ID, Gene symbol, Gene description, and Cellular localization are listed. In the SAGE library names N-normal, D-DCIS, and I-invasive ductal carcinoma.

References:

Cai, L., Huang, H., Blackshaw, S., Liu, J.S., Cepko, C., and Wong, W.H. (2004). Clustering analysis of SAGE data using a Poisson approach. Genome Biol *5*, R51.

Eisen, M.B., Spellman, P.T., Brown, P.O., and Botstein, D. (1998). Cluster analysis and display of genome-wide expression patterns. Proc Natl Acad Sci U S A *95*, 14863-14868.